4. Concluding remarks

Mucosal surface is protected in multiple prudent ways from invasion by pathogens and antigens that induce undesired inflammation (Fig. 3). First, mucosal epithelium covering the associated tissues constitutes physical barriers that are tightly connected by a variety of intercellular adhesive mechanisms such as firm interactions between IELs and IECs and between IECs. Further, mucosal epithelium is covered by thick layers of mucus. Second, responsiveness of mucosal epithelial cells to PAMPs via TLRs are generally suppressed by decrease in the surface expression of TLRs and increase in the intracellular expression of inhibitors that are associated with TLR signaling, thus avoiding induction of unnecessary inflammation as a result of continuous signaling via TLRs. In general, the innate immunity at the mucosa may be negatively regulated and thus maintain the appropriate homeostasis between the host and outside environments.

In contrast, M cells that are located within the epithelium that covers lymphoid or non-lymphoid tissues can behave as a gateway for the transport of antigens and pathogenic microorganisms into the underlying lymphoid follicles or lamina propria, which leads to the initiation of mucosal acquired immunity. DCs located within or in close proximity to

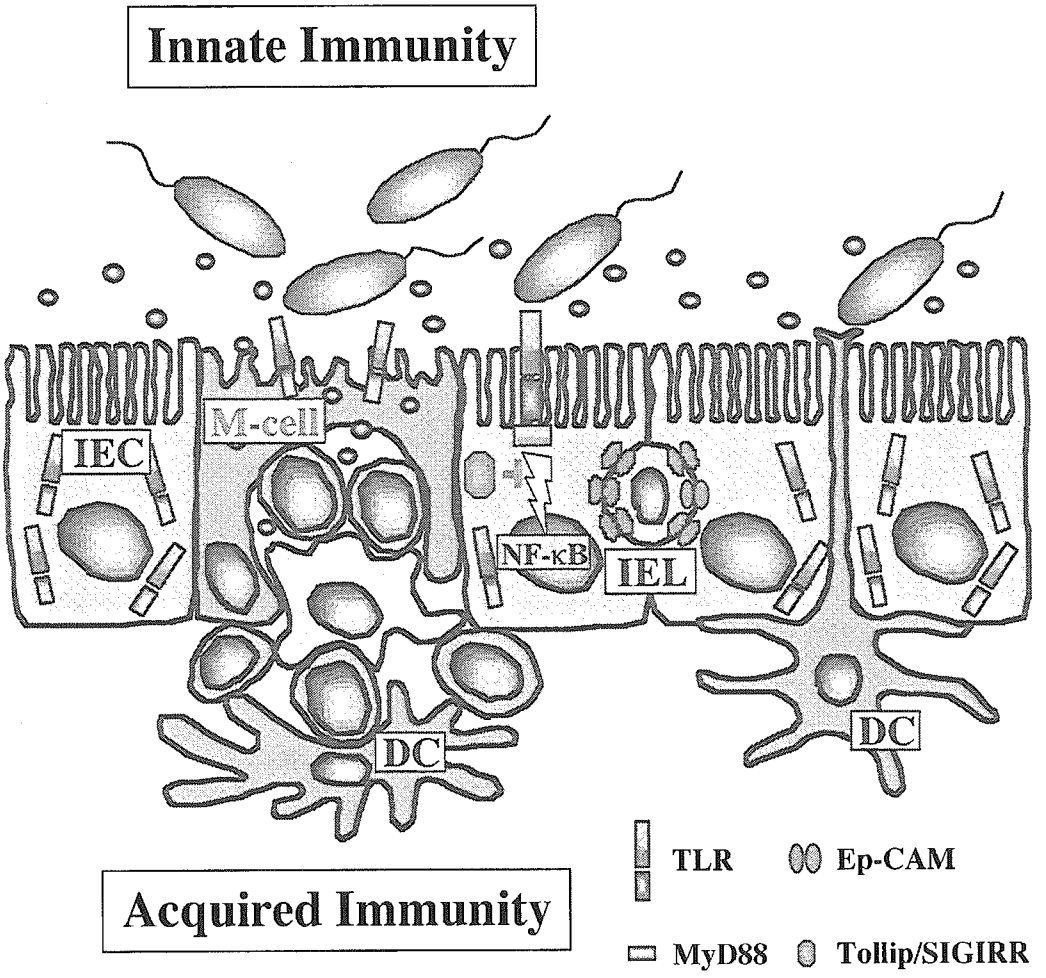

Fig. 3. Dynamic linkage between innate and acquired immunities at mucosal surface.

epithelium also sample antigens and contribute to the induction of acquired immunity. It is interesting to seek out the nature of acquired immunity against antigens taken up by PP-associated M cells, villous M cells, and mucosal DCs located in the different areas of intestinal tract.

It has been reported that DCs express tight junctional proteins to penetrate into epithelium [48] and a variety of TLRs to recognize a wide spectrum of PAMPs [23]. In addition, M cells located within the FAE of swine PP express TLR2 and TLR9 both at the apical and basolateral surfaces [50,51].

Taken all together, these findings suggest that M cells and DCs are key players that bridge innate and acquired immunities at the mucosa.

Acknowledgements

This work was supported by grants from Uehara Memorial Fundation, the Ministry of Education, Science, Sports and Cultures, the Ministry of Health and Welfare and CREST, JST, Japan.

References

[1] B. Creamer, The turnover of the epithelium of the small intestine, Br. Med. Bull. 23 (1967) 226–230.
[2] M. Furuse, et al., Occludin: a novel integral membrane protein localizing at tight junctions, J. Cell Biol. 123 (1993) 1777–1788.
[3] M. Furuse, et al., Claudin-1 and -2: novel integral membrane proteins localizing at tight junctions with no sequence similarity to occludin, J. Cell Biol. 141 (1998) 1539–1550.
[4] K. Morita, et al., Claudin multigene family encoding four-transmembrane domain protein components of tight junction strands, Proc. Natl. Acad. Sci. U. S. A. 96 (1999) 511–516.
[5] J.M. Anderson, C.M. Van Itallie, Tight junctions and the molecular basis for regulation of paracellular permeability, Am. J. Physiol. 269 (1995) G467–G475.
[6] E.E. Schneeberger, R.D. Lynch, Structure, function, and regulation of cellular tight junctions, Am. J. Physiol. 262 (1992) L647–L661.
[7] S. Tsukita, et al., Multifunctional strands in tight junctions, Nat. Rev., Mol. Cell Biol. 2 (2001) 285–293.
[8] M. Takeichi, Cadherin cell adhesion receptors as a morphogenetic regulator, Science 251 (1991) 1451–1455.
[9] S.V. Litvinov, et al., Ep-CAM: a human epithelial antigen is a homophilic cell–cell adhesion molecule, J. Cell Biol. 125 (1994) 437–446.
[10] S.V. Litvinov, et al., Evidence for a role of the epithelial glycoprotein 40 (Ep-CAM) in epithelial cell–cell adhesion, Cell Adhes. Commun. 2 (1994) 417–428.
[11] J. Mestecky, et al., The mucosal immune system, in: W.E. Paul (Ed.), Fundamental Immunology, 5th edn., Lipponcott Williams & Wilkins, Philadelphia, 2003, pp. 965–1020.
[12] K. Fujihashi, et al., Interleukin 2 (IL-2) and interleukin 7 (IL-7) reciprocally induce IL-7 and IL-2 receptors on γδ T-cell receptor-positive intraepithelial lymphocytes, Proc. Natl. Acad. Sci. U. S. A. 93 (1996) 3613–3618.
[13] K. Inagaki-Ohara, et al., Interleukin-15 preferentially promotes the growth of intestinal intraepithelial lymphocytes bearing γδ T cell receptor in mice, Eur. J. Immunol. 27 (1997) 2885–2891.
[14] H. Yang, et al., Intestinal intraepithelial lymphocyte γδ-T cell-derived keratinocyte growth factor modulates epithelial growth in the mouse, J. Immunol. 172 (2004) 4151–4158.
[15] K. Fujihashi, et al., γδ T cell-deficient mice have impaired mucosal immunoglobulin A responses, J. Exp. Med. 183 (1996) 1929–1935.
[16] K. Fujihashi, et al., γδ T cells regulate mucosally induced tolerance in a dose-dependent fashion, Int. Immunol. 11 (1999) 1907–1916.

[17] K.L. Cepek, et al., Adhesion between epithelial cells and T lymphocytes mediated by E-cadherin and the $\alpha_E\beta_7$ integrin, Nature 372 (1994) 190–193.
[18] P.I. Karecla, et al., Recognition of E-cadherin on epithelial cells by the mucosal T cell integrin alpha M290β7 ($\alpha_E\beta_7$), Eur. J. Immunol. 25 (1995) 852–856.
[19] J.M. Higgins, et al., Direct and regulated interaction of integrin $\alpha_E\beta_7$ with E-cadherin, J. Cell Biol. 140 (1998) 197–210.
[20] M.P. Schon, et al., Mucosal T lymphocyte numbers are selectively reduced in integrin α_E (CD103)-deficient mice, J. Immunol. 162 (1999) 6641–6649.
[21] T. Nochi, et al., Biological role of Ep-CAM in the physical interaction between epithelial cells and lymphocytes in intestinal epithelium, Clin. Immunol. 113 (2004) 326–339.
[22] K. Inagaki-Ohara, et al., Intraepithelial lymphocytes express junctional molecules in murine small intestine, Biochem. Biophys. Res. Commun. 331 (2005) 977–983.
[23] R. Medzhitov, C. Janeway Jr., Innate immune recognition: mechanisms and pathways, Immunol. Rev. 173 (2000) 89–97.
[24] D. Yang, et al., Beta-defensins: linking innate and adaptive immunity through dendritic and T cell CCR6, Science 286 (1999) 525–528.
[25] T. Ayabe, et al., Secretion of microbicidal α-defensins by intestinal Paneth cells in response to bacteria, Nat. Immunol. 1 (2000) 113–118.
[26] N. Inohara, et al., Human Nod1 confers responsiveness to bacterial lipopolysaccharides, J. Biol. Chem. 276 (2001) 2551–2554.
[27] S.E. Girardin, et al., Nod2 is a general sensor of peptidoglycan through muramyl dipeptide (MDP) detection, J. Biol. Chem. 278 (2003) 8869–8872.
[28] O. Takeuchi, et al., Differential roles of TLR2 and TLR4 in recognition of Gram-negative and Gram-positive bacterial cell wall components, Immunity 11 (1999) 443–451.
[29] A. Poltorak, et al., Defective LPS signaling in C3H/HeJ and C57BL/10ScCr mice: mutations in Tlr4 gene, Science 282 (1998) 2085–2088.
[30] M. Ueta, et al., Intracellularly expressed TLR2s and TLR4s contribution to an immunosilent environment at the ocular mucosal epithelium, J. Immunol. 173 (2004) 3337–3347.
[31] M.T. Abreu, et al., Decreased expression of Toll-like receptor-4 and MD-2 correlates with intestinal epithelial cell protection against dysregulated proinflammatory gene expression in response to bacterial lipopolysaccharide, J. Immunol. 167 (2001) 1609–1616.
[32] G. Melmed, et al., Human intestinal epithelial cells are broadly unresponsive to Toll-like receptor 2-dependent bacterial ligands: implications for host-microbial interactions in the gut, J. Immunol. 170 (2003) 1406–1415.
[33] Y. Nagai, et al., Essential role of MD-2 in LPS responsiveness and TLR4 distribution, Nat. Immunol. 3 (2002) 667–672.
[34] M.T. Abreu, et al., TLR4 and MD-2 expression is regulated by immune-mediated signals in human intestinal epithelial cells, J. Biol. Chem. 277 (2002) 20431–20437.
[35] F. Randow, B. Seed, Endoplasmic reticulum chaperone gp96 is required for innate immunity but not cell viability, Nat. Cell Biol. 3 (2001) 891–896.
[36] M.W. Hornef, et al., Intracellular recognition of lipopolysaccharide by Toll-like receptor 4 in intestinal epithelial cells, J. Exp. Med. 198 (2003) 1225–1235.
[37] K. Burns, et al., Tollip, a new component of the IL-1RI pathway, links IRAK to the IL-1 receptor, Nat. Cell Biol. 2 (2000) 346–351.
[38] D. Wald, et al., SIGIRR, a negative regulator of Toll-like receptor-interleukin 1 receptor signaling, Nat. Immunol. 4 (2003) 920–927.
[39] C. Garlanda, et al., Intestinal inflammation in mice deficient in Tir8, an inhibitory member of the IL-1 receptor family, Proc. Natl. Acad. Sci. U. S. A. 101 (2004) 3522–3526.
[40] A.T. Gewirtz, et al., Cutting edge: bacterial flagellin activates basolaterally expressed TLR5 to induce epithelial proinflammatory gene expression, J. Immunol. 167 (2001) 1882–1885.
[41] J.M. Otte, et al., Mechanisms of cross hyporesponsiveness to Toll-like receptor bacterial ligands in intestinal epithelial cells, Gastroenterology 126 (2004) 1054–1070.
[42] A. Gebert, et al., M cells in Peyer's patches of the intestine, Int. Rev. Cytol. 167 (1996) 91–159.
[43] C. Borghesi, et al., Rapid appearance of M cells after microbial challenge is restricted at the periphery of the follicle-associated epithelium of Peyer's patch, Lab. Invest. 79 (1999) 1393–1401.

[44] L. Bry, et al., A model of host-microbial interactions in an open mammalian ecosystem, Science 273 (1996) 1380–1383.
[45] M. Yamamoto, et al., Alternate mucosal immune system: organized Peyer's patches are not required for IgA responses in the gastrointestinal tract, J. Immunol. 164 (2000) 5184–5191.
[46] M.H. Jang, et al., Intestinal villous M cells: an antigen entry site in the mucosal epithelium, Proc. Natl. Acad. Sci. U. S. A. 101 (2004) 6110–6115.
[47] P. Kumar, J.F. Timoney, Histology, immunohistochemistry and ultrastructure of the equine tubal tonsil, Anat. Histol. Embryol. 34 (2005) 141–148.
[48] M. Rescigno, et al., Dendritic cells express tight junction proteins and penetrate gut epithelial monolayers to sample bacteria, Nat. Immunol. 2 (2001) 361–367.
[49] J.H. Niess, et al., CX3CR1-mediated dendritic cell access to the intestinal lumen and bacterial clearance, Science 307 (2005) 254–258.
[50] M. Tohno, et al., Toll-like receptor 2 is expressed on the intestinal M cells in swine, Biochem. Biophys. Res. Commun. 330 (2005) 547–554.
[51] T. Shimosato, et al., Toll-like receptor 9 is expressed on follicle-associated epithelia containing M cells in swine Peyer's patches, Immunol. Lett. 98 (2005) 83–89.

nature immunology

© 2005 Nature Publishing Group http://www.nature.com/natureimmunology

Essential function for the kinase TAK1 in innate and adaptive immune responses

Shintaro Sato[1,7], Hideki Sanjo[2,3,7], Kiyoshi Takeda[4], Jun Ninomiya-Tsuji[5], Masahiro Yamamoto[2], Taro Kawai[1], Kunihiro Matsumoto[6], Osamu Takeuchi[1,2] & Shizuo Akira[1,2]

Transforming growth factor-β–activated kinase 1 (TAK1) has been linked to interleukin 1 receptor and tumor necrosis factor receptor signaling. Here we generated mouse strains with conditional expression of a *Map3k7* allele encoding part of TAK1. TAK1-deficient embryonic fibroblasts demonstrated loss of responses to interleukin 1β and tumor necrosis factor. Studies of mice with B cell–specific TAK1 deficiency showed that TAK1 was indispensable for cellular responses to Toll-like receptor ligands, CD40 and B cell receptor crosslinking. In addition, antigen-induced immune responses were considerably impaired in mice with B cell–specific TAK1 deficiency. TAK1-deficient cells failed to activate transcription factor NF-κB and mitogen-activated protein kinases in response to interleukin 1β, tumor necrosis factor and Toll-like receptor ligands. However, TAK1-deficient B cells were able to activate NF-κB but not the kinase Jnk in response to B cell receptor stimulation. These results collectively indicate that TAK1 is key in the cellular response to a variety of stimuli.

Proinflammatory cytokines such as tumor necrosis factor (TNF) and interleukin 1β (IL-1β) have a critical function in innate immune responses by eliciting inflammation[1,2]. The production of proinflammatory cytokines can be induced by various cellular stresses, including pathogenic infection. The initial recognition of invading pathogens is mediated by Toll-like receptors (TLRs), which detect distinct pathogen-associated molecular patterns[2–4]. Stimulation of cells with TLR ligands, IL-1β and TNF activates intracellular signaling pathways leading to the activation of transcription factors such as NF-κB and AP-1 (ref. 1). Activation of AP-1 is mediated by mitogen-activated protein kinases (MAPKs), including Erk, Jnk and p38. Ultimately, these transcription factors initiate expression of genes involved in inflammatory responses. It is well known that TLRs and IL-1 receptor (IL-1R) activate similar signaling pathways[3]. The cytoplasmic portions of TLRs and IL-1Rs contain the Toll–IL-1R homology domain. Ligand stimulation recruits MyD88, a Toll–IL-1R homology domain–containing adaptor protein, to the Toll–IL-1R homology domain of the receptor. Subsequently, IL-1R-associated kinases (IRAKs) are recruited and phosphorylated, and then they interact with TNF receptor (TNFR)–associated factor 6 (TRAF6)[3]. TRAF6 comprises an N-terminal RING finger domain, which has been found in a family of E3 ubiquitin ligases[5]. It has been proposed that a dimeric ubiquitin-conjugating enzyme complex composed of Ubc13 and Uev1A, together with TRAF6, can catalyze the formation of a K63-linked polyubiquitin chain[5,6]. The ubiquitination is responsible for the activation of IκB kinases (IKKs). Subsequently, phosphorylated IκB undergoes degradation by the ubiquitin-proteosome system, and NF-κB translocates into nucleus and triggers transcription of target genes[7]. Simultaneously, MAPKs are activated 'downstream' of TRAF6 by activating MAPK kinase 6 (MKK6)[8]. In the TNFR signaling pathway, ligand stimulation leads to the recruitment of adaptor proteins, including TRADD, TRAF2 and RIP1, to the receptor complex. Genetic studies have shown that TRAF2 is responsible for MAPK activation, whereas RIP1 is required for NF-κB activation[1,4].

Transforming growth factor-β–activated kinase 1 (TAK1), a member of the MAPK kinase kinase (MAPKKK) family, was originally identified as a kinase involved in TGF-β signaling[9]. TAK1 is evolutionally conserved, and drosophila TAK1 is critical for antibacterial innate immunity[10]. In addition, TAK1 functions as an 'upstream' signaling molecule of NF-κB and MAPKs in IL-1R signaling pathways. Furthermore, TAK1 is activated by TNF, bacterial lipopolysaccharide (LPS) and latent membrane protein 1 from Epstein-Barr virus[11–13]. Activated TAK1 is recruited to TRAF6 and TRAF2 complexes in response to IL-1R and TNFR stimulation, respectively. A point mutation in the gene encoding TAK1 altering its ATP-binding domain abolishes both its kinase activity and its ability to activate IKKs and MAPKs[8]. TAK1 forms a complex with its association partners, TAB1, TAB2 and TAB3 (refs. 14–17). It has been proposed that TRAF6-mediated K63-linked

[1]Akira Innate Immunity Project, Exploratory Research for Advanced Technology, Japan Science and Technology Agency and [2]Department of Host Defense, Research Institute for Microbial Diseases, Osaka University, Suita, Osaka 565-0871, Japan. [3]Lymphocyte Differentiation, RIKEN Research Center for Allergy and Immunology, Yokohama, Kanagawa 230-0045, Japan. [4]Department of Molecular Genetics, Medical Institute of Bioregulation, Kyushu University, Fukuoka 812-8582, Japan. [5]Department of Environmental and Molecular Toxicology, North Carolina State University, Raleigh, North Carolina 27695-7633, USA. [6]Department of Molecular Biology, Graduate School of Science, Nagoya University, Nagoya, 464-8602, Japan. [7]These authors contributed equally to this work. Correspondence should be addressed to S.A. (sakira@biken.osaka-u.ac.jp).

Received 4 April; accepted 10 August; published online 25 September 2005; doi:10.1038/ni1255

polyubiquitination is required for the activation of TAK1. Activated TAK1 complex phosphorylates IKKs and MKK6, which activate NF-κB and MAPKs, respectively. *In vitro* studies have shown that expression of TAK1 together with TAB1 enhances activation of a NF-κB reporter gene[8]. Reciprocally, 'knockdown' of *Map3k7*, the gene encoding TAK1, in HeLa cells by RNA interference results in abrogation of IL-1β- and TNF-induced NF-κB activation[11].

The function of TAB1 and TAB2 has been assessed by examination of mouse models lacking genes encoding these proteins. Analysis of TAB2-deficient mice has shown that TAB2 is dispensable for IL-1R signaling[18]. Studies of TAB1-deficient mice have shown that TAB1 is involved in TGF-β signaling[19]. However, the function of TAB1 in IL-1R signaling *in vivo* has not been described. Therefore, it is still unclear whether TAK1-binding proteins are essential for TAK1 activation or if the TAK1 complex itself is dispensable for NF-κB and MAPK signaling *in vivo*. Although the function of TAK1 in drosophila innate immune response has been studied extensively[10], its involvement in the mammalian TLR system is not well understood.

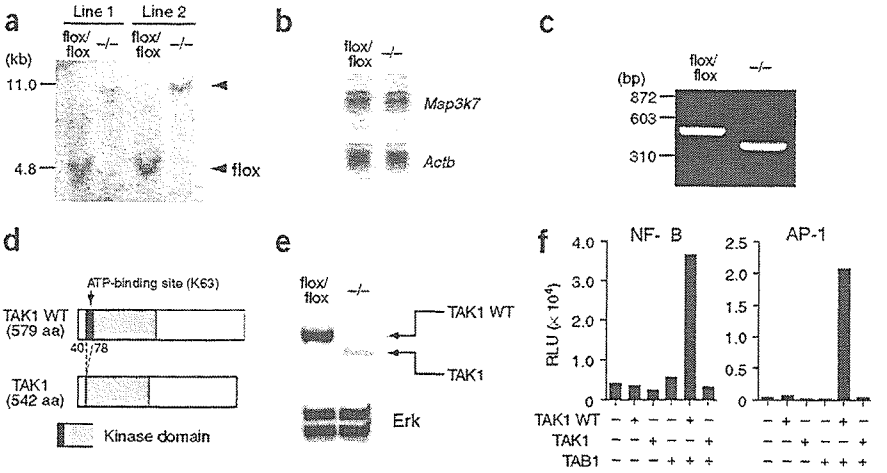

Figure 1 Establishment of *Map3k7* $^{-/-}$ MEFs. **(a)** Southern blot analysis of genomic DNA from *Map3k7* $^{-/-}$ and control *Map3k7*$^{flox/flox}$ (flox/flox) MEFs, after digestion with *Xba*I and *Eco*RI (probe, **Supplementary Fig. 1** online). Right and left margins, positions of 11.0-kb floxed and 4.8-kb Δ fragments. **(b)** RNA blot analysis of total RNA prepared from *Map3k7* $^{-/-}$ and *Map3k7*$^{flox/flox}$ MEFs. The 5′ ends of *Map3k7* and *Actb* (encoding β-actin) cDNA fragments were used as probes. **(c)** RT-PCR analysis of total RNA from MEFs, using primers amplifying the encoding region of exons 1–3. **(d)** Predicted structure of TAK1Δ, which lacks the ATP-binding site (arrow) required for kinase activity. WT, wild-type; aa, amino acids. **(e)** Immunoblot analysis of lysates of *Map3k7* $^{-/-}$ and *Map3k7*$^{flox/flox}$ MEFs (antibodies, right margin). **(f)** NF-κB- or AP-1-dependent reporter assay. HEK293 cells were transiently transfected with plasmids (below graphs) plus an NF-κB-dependent (left) or an AP-1-dependent (right) luciferase reporter plasmid. Then, 36 h after transfection, luciferase activity (RLU, relative light units) in whole-cell lysates was measured. Data are representative of three independent experiments.

Here we have examined the function of TAK1 *in vivo* by gene targeting using the Cre-*lox*P system. *Map3k7* deficiency in the germline resulted in early embryonic death. Therefore, we generated TAK1-deficient (*Map3k7* $^{-/-}$) mouse embryonic fibroblasts (MEFs) by *in vitro* introduction of Cre in MEFs homozygous for *lox*P-flanked (floxed) *Map3k7* alleles (*Map3k7*$^{flox/flox}$). First we examined the function of TAK1 in IL-1R and TNF signaling using TAK1-deficient MEFs and found that TAK1 was required for IL-1β- and TNF-induced NF-κB and Jnk activation as well as cytokine production. Next we analyzed TLR- and B cell receptor (BCR)–mediated signaling using B cells as a model. B cell–specific deletion of TAK1 resulted in considerably impaired B cell activation in response to various stimuli, including nonmethylated CpG DNA (a ligand for TLR9), polyinosine-polycytidylic acid (poly(I:C); a ligand for TLR3), LPS (a ligand for TLR4), CD40 and BCR crosslinking. Furthermore, LPS and CpG DNA failed to activate Jnk and NF-κB in TAK1-deficient B cells, indicating that TAK1 is essential for activating these signaling pathways. Notably, although BCR crosslinking on TAK1-deficient B cells also demonstrated defective Jnk activation, activation of NF-κB as well as expression of NF-κB target genes was comparable to that of wild-type cells. Our conditional TAK1-deficient mouse model therefore shows that TAK1 is essential for TLR, IL-1R, TNFR and BCR cellular responses and signaling pathways leading to the activation of Jnk and/or NF-κB.

RESULTS

Map3k7 $^{-/-}$ mice die early *in utero*

To investigate the function of TAK1 *in vivo*, we generated mice with conditional deletion of a *Map3k7* allele. We constructed a gene-targeting vector by placing *lox*P sites flanking exon 2 of mouse *Map3k7*, which encodes a part of the kinase domain of TAK1, including its ATP-binding site (Lys63), and a floxed neomycin-resistance gene into an intron 1 of *Map3k7* (**Supplementary Fig. 1** online). To generate mice heterozygous for deletion of this *Map3k7* allele (*Map3k7*$^{+/-}$ mice), we mated mice with one floxed allele and one wild-type allele (*Map3k7*$^{flox/+}$ mice) with a mice of a transgenic line expressing Cre in germ cells. We confirmed deletion of *Map3k7* in the germline by Southern blot analysis (**Supplementary Fig. 1** online). Of about 90 newborn pups obtained by intercrossing *Map3k7*$^{+/-}$ mice, we obtained no *Map3k7* $^{-/-}$ mice, indicating that the TAK1 deficiency is embryonically lethal (**Supplementary Fig. 1** online). Although we identified *Map3k7* $^{-/-}$ embryos on embryonic day 9.5 (E9.5) in normal mendelian ratios, we found no *Map3k7* $^{-/-}$ fetuses in decidua containing normal fetuses after E10.5 (**Supplementary Fig. 1** online).

Establishment of *Map3k7* $^{-/-}$ MEFs

As *Map3k7* $^{-/-}$ MEFs obtained from E9.5 embryos failed to grow, we prepared MEFs from *Map3k7*$^{flox/flox}$ mice. To generate TAK1-deficient MEFs, we excised the floxed genomic fragment by retroviral expression of Cre protein together with green fluorescent protein (GFP). We sorted GFP$^+$ cells by flow cytometry. Southern blot analysis showed that complete conversion of the floxed allele to the deleted (Δ) allele was achieved in GFP$^+$ cells from two lines of *Map3k7* $^{-/-}$ MEFs (**Fig. 1a**). However, we detected *Map3k7* transcripts in *Map3k7* $^{-/-}$ MEFs with same migration and intensity as that of *Map3k7*$^{flox/flox}$ MEFs (**Fig. 1b**). RT-PCR analysis using primers to amplify the region of exons 1–3 showed a product with faster migration in *Map3k7* $^{-/-}$ cells (**Fig. 1c**). Nucleotide sequence analysis of the product showed that the deletion of exon 2 from TAK1 cDNA was in-frame, indicating that Cre-mediated deletion led to the production of an altered TAK1 (TAK1Δ; **Fig. 1d**). Immunoblot analysis showed weak expression of TAK1Δ in *Map3k7* $^{-/-}$ cells (**Fig. 1e**). To confirm that TAK1Δ lacked

© 2005 Nature Publishing Group http://www.nature.com/natureimmunology

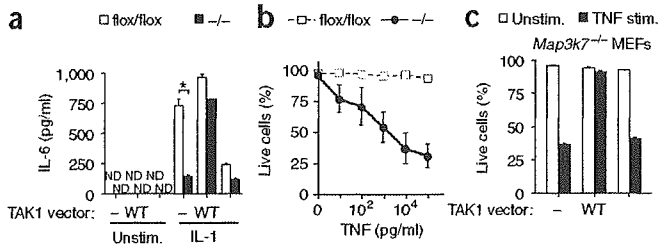

Figure 2 Impaired responses to IL-1β and TNF in *Map3k7* $^{-/-}$ MEFs. (**a**) IL-6 production by MEFs. Control *Map3k7* $^{flox/flox}$ and *Map3k7* $^{-/-}$ MEFs were transfected with empty ( ), wild-type TAK1 (WT) or TAK1Δ (Δ) plasmid, and then were stimulated for 24 h with 10 ng/ml of IL-1β. IL-6 in the culture medium was measured by ELISA. Data are mean ± s.d. of triplicate samples of one representative from three independent experiments. *, $P < 0.005$, versus TAK1-deficient cells (Student's *t*-test). ND, not detected. (**b**) Viability of control and *Map3k7* $^{-/-}$ MEFs treated for 24 h with various concentrations of TNF (horizontal axis), assessed by annexin V–indocarbocyanine staining. Three independent experiments were done in triplicate. Data are mean ± s.d. percentage of viable cells after treatment relative to untreated control. (**c**) Viability of control and *Map3k7* $^{-/-}$ MEFs left untransfected or transfected with wild-type or mutated TAK1 and were left unstimulated (Unstim.) or were stimulated for 24 h with 10 ng/ml of TNF (TNF stim.). Data represent mean ± s.d. for percentage of viable cells after treatment relative to untreated control.

the ability to activate NF-κB and AP-1, we did a reporter assay. Overexpression of wild-type TAK1, but not TAK1Δ, together with TAB1 in human embryonic kidney 293 (HEK293) cells activated NF-κB and AP-1, indicating that TAK1Δ was nonfunctional because it lacked an ATP-binding site (**Fig. 1f**).

TAK1 is required for IL-1β and TNF responsiveness

We first examined responses to IL-1β and TNF. We stimulated *Map3k7* $^{-/-}$ and control *Map3k7* $^{flox/flox}$ MEFs with IL-1β and measured IL-6 production by enzyme-linked immunosorbent assay (ELISA). Production of IL-6 was impaired considerably in *Map3k7* $^{-/-}$ MEFs compared with that in control cells (**Fig. 2a**). Moreover, re-expression of wild-type TAK1 but not TAK1Δ in *Map3k7* $^{-/-}$ MEFs restored IL-6 production in response to IL-1β.

As NF-κB activation is required for survival of MEFs after exposure to TNF, we next compared the viability of TNF-stimulated cells. TNF stimulation induced cell death in *Map3k7* $^{-/-}$ MEFs in a dose-dependent way (**Fig. 2b**). In contrast, *Map3k7* $^{flox/flox}$ MEFs were viable after TNF stimulation. The TNF-induced cell death noted in *Map3k7* $^{-/-}$ MEFs was circumvented by expression of wild-type TAK1 but not TAK1Δ (**Fig. 2c**). These results indicate that TAK1 is required for IL-1β- and TNF-mediated cellular responses.

We further examined the activation of signaling molecules. In both *Map3k7* $^{flox/flox}$ and *Map3k7* $^{-/-}$ MEFs, IRAK-1 was phosphorylated, ubiquitinated and degraded in response to IL-1β, indicating that TAK1 was not involved in IRAK-1 activation (**Fig. 3a**). Induction of NF-κB DNA binding and degradation of IκBα in response to IL-1β and TNF were compromised in *Map3k7* $^{-/-}$ MEFs (**Fig. 3b**). Furthermore, activation of Jnk and p38 in response to IL-1β and TNF in *Map3k7* $^{-/-}$ MEFs was also impaired (**Fig. 3c**). Thus, TAK1 was required for NF-κB, Jnk and p38 activation in response to IL-1β and TNF in MEF cells.

Generation of mice with B cell–specific TAK1 deficiency

Although the involvement of TAK1 in the IL-1β signaling has been studied extensively, its involvement in the TLR signaling pathway is less understood. Because B cells express various TLRs and respond to their ligands to proliferate, we generated mice with B cell–specific TAK1 deficiency by breeding *Map3k7* $^{flox/}$ mice with mice carrying the *Cre* transgene under control of the *Cd19* promoter (*Cd19* $^{Cre/+}$). Southern blot analysis showed almost complete Cre-mediated deletion of *Map3k7* in B cells from *Cd19* $^{Cre/+}$*Map3k7* $^{flox/}$ mice (**Supplementary Fig. 2** online). We also checked deletion of TAK1 in purified B cells by immunoblot analysis and confirmed that the expression of wild-type TAK1 was considerably reduced in B cells from *Cd19* $^{Cre/+}$*Map3k7* $^{flox/}$ mice (**Supplementary Fig. 2** online).

TAK1 deficiency impairs B-1 B cell development

We investigated whether B cell–specific TAK1 deficiency affected lymphopoiesis. The population of B cell precursors in the bone marrow was comparable in *Cd19* $^{Cre/+}$*Map3k7* $^{flox/+}$ and *Cd19* $^{Cre/+}$*Map3k7* $^{flox/}$ mice (**Fig. 4a**). The ratio of B cells to T cells, the expression of surface immunoglobulin M (IgM) and IgD on mature splenic B cells and the numbers of marginal zone B cells (IgM$^+$CD23$^-$ CD21$^+$) were also comparable for *Cd19* $^{Cre/+}$*Map3k7* $^{flox/+}$ and *Cd19* $^{Cre/+}$*Map3k7* $^{flox/}$ splenocyte samples (**Fig. 4b**). However, the B220$^+$CD5$^+$ B-1 B cell population was reduced in the peritoneal cavities of *Cd19* $^{Cre/+}$*Map3k7* $^{flox/}$ mice (**Fig. 4c**). These results indicate that TAK1 was required for the development of B-1 B cells but not of splenic follicular and marginal zone B cells.

TAK1 is required for the TLR signaling in B cells

B cells become active and progress through the cell cycle in response to TLR ligands such as LPS, CpG DNA and poly(I:C). Although *Cd19* $^{Cre/+}$*Map3k7* $^{flox/+}$ B cells proliferated in response to all TLR

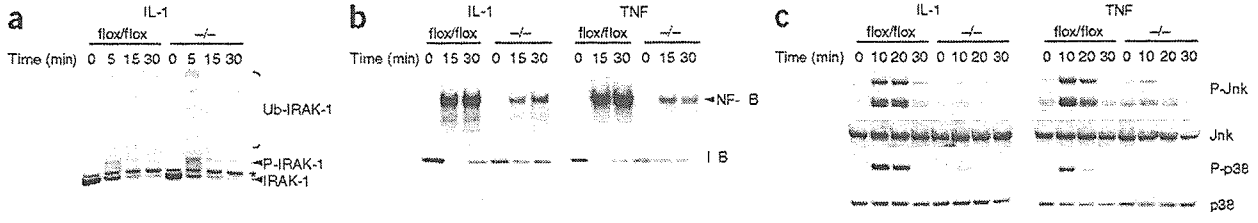

Figure 3 Impaired activation of NF-κB and MAPKs in response to IL-1β and TNF in TAK1-deficient cells. (**a**) Immunoblot of IRAK-1 in whole-cell lysates of control and *Map3k7* $^{-/-}$ MEFs left untreated or treated with 10 ng/ml of IL-1β (time, above lanes). Ub-, ubiquitinated; P-, phosphorylated; *, nonspecific band. (**b**) Control and *Map3k7* $^{-/-}$ MEFs were treated with IL-1β (10 ng/ml) or TNF (10 ng/ml) for various times (above lanes). The NF-κB DNA-binding activity in nuclear extracts was determined by EMSA (top). Degradation of IκBα whole-cell lysates was detected by immunoblot with anti-IκBα (bottom). (**c**) Phosphorylation of Jnk and p38 (P-Jnk and P-p38, respectively) in whole-cell lysates of control and *Map3k7* $^{-/-}$ MEFs treated with IL-1β (10 ng/ml) or TNF (10 ng/ml) for various times (above lanes), assessed by immunoblot with phosphorylation-specific antibodies. Jnk and p38, loading controls. All results are representative of three different experiments.

© 2005 Nature Publishing Group http://www.nature.com/natureimmunology

ligands tested, the proliferation of B cells from *Cd19*$^{Cre/+}$*Map3k7*$^{flox/}$ mice was considerably impaired (**Fig. 5a**). In addition, follicular and marginal zone B-2 cells purified from *Cd19*$^{Cre/+}$*Map3k7*$^{flox/}$ spleens had impaired proliferative responses to LPS and/or CpG DNA (**Supplementary Fig. 3** online). We also investigated cell cycle profiles by staining with bromodeoxyuridine (BrdU) and 7-amino-actinomycin D. Unlike *Cd19*$^{Cre/+}$*Map3k7*$^{flox/+}$ B cells, whose cell cycles progressed into S phase, *Cd19*$^{Cre/+}$*Map3k7*$^{flox/}$ B cells showed impaired entry to S phase after treatment with LPS and CpG DNA (**Fig. 5b**). These results indicate that TAK1 is responsible for TLR-mediated responses in B cells.

We next examined whether TAK1 deficiency influences the viability of B cells. When control B cells were cultured *ex vivo* without mitogens, 50% of the cells spontaneously underwent apoptosis within 12 h of culture (**Fig. 5c**). Stimulation with LPS or CpG DNA prevented the execution of apoptosis in control B cells. In contrast, prevention of cell death in response to LPS or CpG DNA was impaired in *Cd19*$^{Cre/+}$*Map3k7*$^{flox/}$ B cells. These results indicate that TAK1 is critical for TLR ligand–mediated prevention of B cell death.

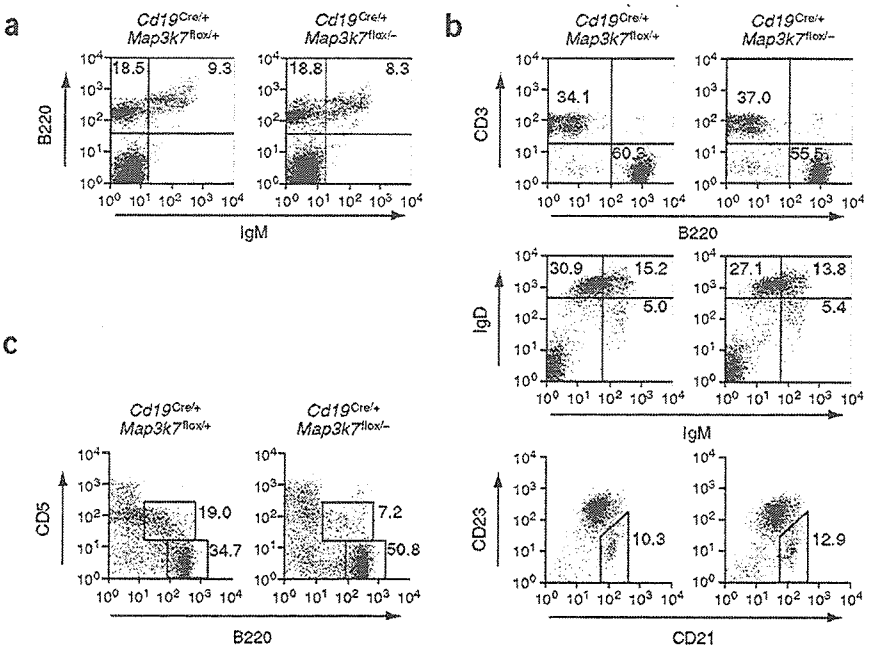

Figure 4 B cell development in *Cd19*$^{Cre/+}$*Map3k7*$^{flox/}$ mice. Flow cytometry of B cell development in the bone marrow (**a**), splenic (**b**) and peritoneal (**c**) B cells from 8-week-old *Cd19*$^{Cre/+}$*Map3k7*$^{flox/+}$ and *Cd19*$^{Cre/+}$*Map3k7*$^{flox/}$ mice. Numbers in the quadrants or beside boxed areas indicate the percentage of positive cells in that region. Results are representative of four different experiments.

We further analyzed the upregulation of surface activation markers in response to TLR stimuli. In accordance with defects in cell proliferation and apoptosis inhibition, *Cd19*$^{Cre/+}$*Map3k7*$^{flox/}$ B cells stimulated with LPS or CpG DNA showed impaired upregulation of cell surface CD69 and CD86 expression (**Fig. 5d**). It has been reported that CpG DNA induces IL-6 production from human naive B cells[20]. In mouse splenic B cells, IL-6 was produced in response to CpG DNA and LPS (**Fig. 5e**). However, IL-6 production by *Cd19*$^{Cre/+}$*Map3k7*$^{flox/}$ B cells in response to either LPS or CpG DNA was less than that of control *Cd19*$^{Cre/+}$*Map3k7*$^{flox/+}$ B cells.

We also assessed TLR-induced activation of signaling pathways in TAK1-deficient B cells. In *Cd19*$^{Cre/+}$*Map3k7*$^{flox/+}$ B cells, stimulation with LPS or CpG DNA resulted in degradation of IκBα and activation of NF-κB DNA-binding activity (**Fig. 5f,g**). In contrast, IκBα degradation and NF-κB DNA-binding activity in response to LPS and CpG DNA were reduced considerably in *Cd19*$^{Cre/+}$*Map3k7*$^{flox/}$ B cells. In addition, activation of Jnk, p38 and Erk was impaired in LPS- and CpG DNA–stimulated *Cd19*$^{Cre/+}$*Map3k7*$^{flox/}$ B cells (**Fig. 5h**). These findings indicate that TAK1 is critical for TLR-mediated B cell activation and signaling.

Requirement for TAK1 for activation of BCR signaling

BCR signaling also activates NF-κB and MAPKs, leading to B cell activation. Crosslinking of BCRs induces activation of tyrosine kinases, an increase in intracellular calcium and activation of protein kinase C-β[21]. A complex of the signaling molecules CARD11 (also known as CARMA1), Bcl10 and MALT1 (also known as paracaspase) then transduces signals to NF-κB and MAPKs downstream of protein kinase C-β[22]. It has also been proposed that TAK1 is involved in T cell receptor signaling downstream of TRAF6 to activate NF-κB[23]. However, the function of TAK1 in BCR signaling is unknown. We therefore analyzed activation of TAK1-deficient B cells in response to BCR crosslinking. Inactivation of TAK1 considerably impaired the proliferation of purified B cells in response to BCR and CD40 stimulation, similar to their response to TLR ligands, indicating that TAK1 is involved in the signaling pathways used by BCRs and CD40 (**Fig. 6a** and **Supplementary Fig. 3** online). Furthermore, *Cd19*$^{Cre/+}$*Map3k7*$^{flox/}$ B cells showed impaired entry to S phase and impaired enhancement of cell survival after BCR crosslinking compared with that of control *Cd19*$^{Cre/+}$*Map3k7*$^{flox/+}$ B cells (**Fig. 6b,c**). In contrast, BCR stimulation induced almost similar upregulation of CD69 and CD86 in control and *Cd19*$^{Cre/+}$*Map3k7*$^{flox/}$ B cells (**Fig. 6d**).

We next examined the activation of BCR-mediated signaling pathways in further detail. Tyrosine phosphorylation of cytoplasmic proteins in response to BCR stimulation was not altered in *Cd19*$^{Cre/+}$*Map3k7*$^{flox/}$ B cells (**Fig. 6e**). Unexpectedly, BCR-mediated activation of NF-κB was not impaired in TAK1-deficient B cells (**Fig. 6f,g**). Among MAPKs, activation of Jnk but not p38 or Erk was considerably impaired (**Fig. 6h**). These data demonstrate that the requirement for TAK1 in NF-κB activation differs depending on the stimuli, whereas TAK1 functions as an essential activator of Jnk in response to a variety of stimuli.

To further elucidate how TAK1 regulates BCR-mediated proliferative responses, we investigated BCR-induced gene expression profiles by microarray analysis. The BCR-mediated expression of genes involved in cell cycling and survival was not impaired in *Cd19*$^{Cre/+}$*Map3k7*$^{flox/}$ B cells (**Supplementary Table 1** online). The upregulation of cyclin D2 protein as well as mRNA was comparable in BCR-stimulated control and TAK1-deficient B cells (**Supplementary Fig. 4** and **Supplementary Table 1** online). However, the downregulation of p27^{Kip1} expression was impaired in *Cd19*$^{Cre/+}$*Map3k7*$^{flox/}$ B cells, suggesting that G1-S progression was impaired at the level of p27 expression (**Supplementary Fig. 4** online).

Bcl10 and CARD11 are crucial for BCR-induced Jnk and NF-κB activation. In contrast, MALT1 is required for the activation of NF-κB

© 2005 Nature Publishing Group http://www.nature.com/natureimmunology

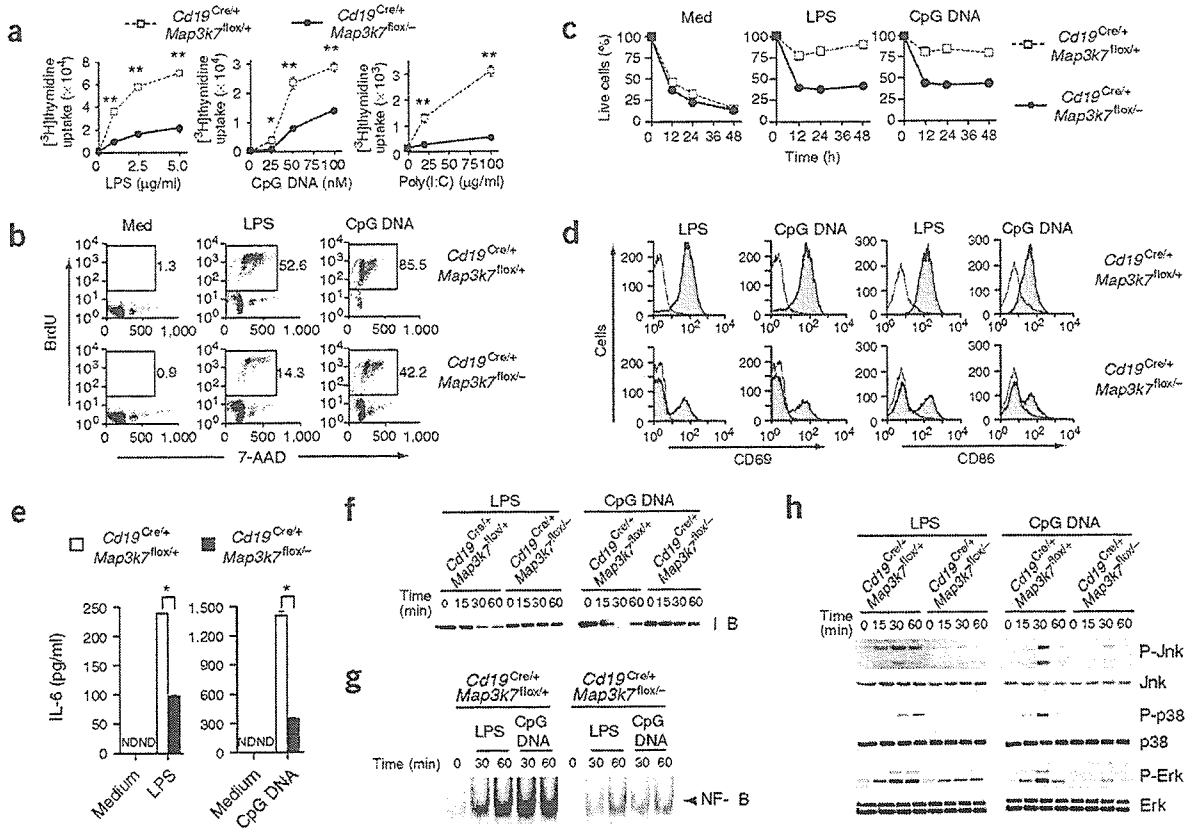

Figure 5 Impaired B cell activation in response to TLR ligands in $Cd19^{Cre/+}Map3k7^{flox/}$ mice. (**a**) Proliferation of purified splenic B cells treated 48 h with various stimuli (horizontal axes), assessed by [^{3}H]thymidine incorporation. Data are mean ± s.d. of triplicate cultures. *, $P < 0.05$ and **, $P < 0.005$, versus TAK1-deficient cells (Student's *t*-test). (**b**) Cell cycle profiles of B cells left untreated (Med) or after *in vitro* stimulation with 5 μg/ml of LPS or 100 nM CpG DNA. Cells were labeled with BrdU and were analyzed by flow cytometry 24 h after stimulation. Numbers beside boxed areas indicate percentage of cells in S phase. (**c**) Defective survival of $Cd19^{Cre/+}Map3k7^{flox/}$ cells. B cells were stimulated with 5 μg/ml of LPS or 100 nM CpG DNA. Viability of cells was assessed by staining with annexin V–indocarbocyanine followed by flow cytometry (time, horizontal axes). (**d**) Surface expression of activation markers. B cells were left unstimulated (open) or were stimulated for 24 h with 5 μg/ml of LPS or 100 nM CpG DNA (filled). Cells were then stained with anti-CD69 or anti-CD86. (**e**) ELISA of IL-6 production by B cells stimulated with LPS (20 μg/ml) or CpG DNA (2 μM). Data are mean ± s.d. of triplicate samples of one representative of three independent experiments. *, $P < 0.005$, versus TAK1-deficient cells (Student's *t*-test). (**f**) Immunoblot of IκBα degradation by B cells in response to LPS (20 μg/ml) or CpG DNA (2 μM). (**g**) EMSA of NF-κB DNA-binding activity in nuclear extracts of purified splenic B cells treated (time, above lanes) with LPS (20 μg/ml) or CpG DNA (2 μM). (**h**) Immunoblot of lysates of B cells stimulated (time, above lanes) with LPS (20 μg/ml) or CpG DNA (2 μM). Antibodies, right margin. All results are representative of three different experiments.

© 2005 Nature Publishing Group http://www.nature.com/natureimmunology

but not Jnk downstream of Bcl10 in BCR signaling. Mice lacking Bcl10, CARD11 or MALT1 are reported to have defects in the development of B-1 B cells and B cell activation. That prompted us to hypothesize that TAK1 may be recruited to the Bcl10 complex to activate Jnk. Therefore, we examined the association of TAK1 and Bcl10 using the human B cell line WEHI-231. When the cells were stimulated with antibody to IgM (anti-IgM), Bcl10 was immunoprecipitated together with TAK1 and with CARD11 (**Fig. 6i**). In contrast, TAK1 failed to precipitate together with Bcl10 in LPS-stimulated cells (**Fig. 6i**). These results suggest that TAK1 is recruited to the Bcl10 complex after BCR stimulation and is involved in Bcl10-mediated Jnk activation in B cells.

TAK1 is required for *in vivo* immune responses

We further investigated the involvement of TAK1 in humoral immune responses. The serum immunoglobulin concentrations of all isotypes except IgM were lower in $Cd19^{Cre/+}Map3k7^{flox/}$ B cells than in $Cd19^{Cre/+}Map3k7^{flox/+}$ B cells (**Fig. 7a**). To induce humoral immune responses, we challenged $Cd19^{Cre/+}Map3k7^{flox/}$ and littermate $Cd19^{Cre/+}Map3k7^{flox/+}$ mice with the T cell–dependent antigen nitrophenol conjugated to chicken γ-globulin or with the T cell–independent type II antigen trinitrophenol conjugated to Ficoll. The production of antigen-specific IgG1 in response to the T cell–dependent antigen was considerably impaired in $Cd19^{Cre/+}Map3k7^{flox/}$ mice compared with that of control $Cd19^{Cre/+}Map3k7^{flox/+}$ mice, whereas IgM titers were similar in both groups of mice (**Fig. 7b**). Similarly, IgG3 production of $Cd19^{Cre/+}Map3k7^{flox/}$ mice injected with trinitrophenol-Ficoll was impaired compared with that of control mice (**Fig. 7c**). This might have been due to the reduction in B-1 B cells in $Cd19^{Cre/+}Map3k7^{flox/}$ mice, as B-1 B cells are the chief mediators of the T cell–independent response[24]. Impaired activation of B cells may also contribute to the defect in the istype switching. These results show that TAK1 is required for the appropriate induction of humoral immune responses.

DISCUSSION

Here we generated TAK1-deficient mice and a mouse strain with conditional expression of a *Map3k7* allele. *In vitro* studies have

© 2005 Nature Publishing Group http://www.nature.com/natureimmunology

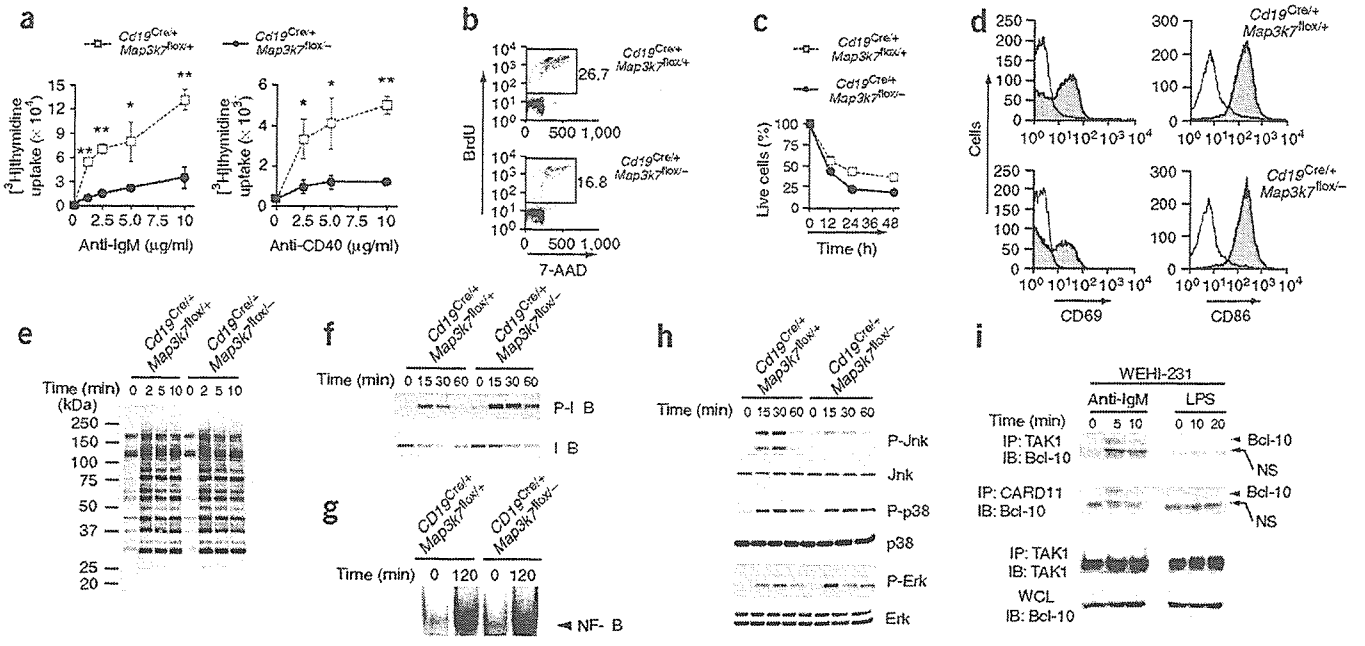

Figure 6 Impaired B cell activation by crosslinking of BCRs in *Cd19*$^{Cre/+}$*Map3k7*$^{flox/}$ mice. (**a**) Proliferation of purified splenic B cells stimulated for 48 h (stimuli, horizontal axes), assessed by [^{3}H]thymidine incorporation. Data are mean ± s.d. of triplicate cultures. *, $P < 0.05$ and **, $P < 0.005$, versus TAK1-deficient cells (Student's *t*-test). (**b**) Cell cycle profiles of B cells stimulated with 5 μg/ml of anti-IgM. Cells were labeled with BrdU and were analyzed by flow cytometry 24 h after stimulation. Numbers beside boxed areas indicate percentages of cells in S phase. (**c**) Viability of B cells stimulated with 5 μg/ml of anti-IgM, assessed by staining with annexin V–indocarbocyanine followed by flow cytometry (time, horizontal axis). (**d**) Flow cytometry of purified splenic B cells left unstimulated (open) or stimulated for 24 h with 5 μg/ml of anti-IgM (filled) and then stained with anti-CD69 or anti-CD86. (**e**) Total tyrosine phosphorylation of B cells stimulated with 20 μg/ml of anti-IgM (time, above lanes). (**f**) Immunoblot of IκBα degradation in B cells in response to 20 μg/ml of anti-IgM. (**g**) EMSA of NF-κB DNA-binding activity in nuclear extracts from purified splenic B cells stimulated for 2 h with 20 μg/ml of anti-IgM. (**h**) MAPK activation in BCR-stimulated B cells stimulated with 20 μg/ml of anti-IgM (time, above lanes). (**i**) Association between TAK1 and Bcl10. WEHI-231 cells (1.5 10^8) were stimulated with 20 μg/ml of anti-IgM or 20 μg/ml of LPS (time, above lanes); cell lysates were immunoprecipitated (IP) with anti-TAK1 or anti-CARD11 and immunoprecipitates or whole-cell lysates (WCL) were analyzed by immunoblot (IB; antibodies, left margin). All results are representative of three different experiments. NS, nonspecific band.

suggested that TAK1 has an important function in IL-1R and TNFR signaling by forming a complex with TAB1 and TAB2 (refs. 11,14,15). However, mice lacking TAB2 have normal IL-1β responses[18]. The function of TAB1 in the IL-1R signaling is still unclear, although involvement TAB1 in TGF-β signaling has been reported in studies of TAB1-deficient mice[19]. It is possible TAB3, a homolog of TAB2, functions redundantly in TAB2-deficient mice[16,17,25,26]. In contrast, TAK1-deficient MEFs showed considerably impaired responses, including activation of NF-κB and MAPKs in response to IL-1β stimulation. However, IL-1β-induced production of IL-6 or activation of NF-κB was not completely abrogated in TAK1-deficient MEFs, indicating IL-1R activates both TAK1-dependent and TAK1-independent signaling pathways.

The involvement of TAK1 in TNFR signaling is controversial. Initially, TAK1 was reported to bind TRAF6 but not TRAF2, an important mediator of TNFR signaling[8]. However, other *in vitro* studies have shown that TAK1 regulates TNF-induced NF-κB activation[11,26]. Our results have demonstrated that TAK1 is critical for activation of both NF-κB and MAPKs in response to TNF. In addition, stimulation with TNF alone induced massive cell death in *Map3k7* $^{/}$ MEFs. In wild-type cells, TNF stimulation activates NF-κB and MAPK pathways, which mediate cell survival and proliferation by expressing target genes such as those encoding inhibitor of apoptosis and Bcl-2 family members[1]. TNF simultaneously activates the apoptotic pathway by recruiting Fas-associated death domain and caspase 8, followed by activation of caspase 3. This pathway does not require protein synthesis[1]. It is believed that the balance between life and death signals determines the fate of the cell. TNF kills wild-type cells when protein synthesis is inhibited. Given that TNF-induced NF-κB and MAPK activation was considerably impaired in *Map3k7* $^{/}$ MEFs, cells lacking TAK1 might fail to induce survival genes that protect cells from TNF-induced cell death.

The function of TAK1 in TLR signaling is less well understood. As B cells express various TLRs and are activated in response to pathogen-associated molecular patterns, we examined the involvement of TAK1 in TLR signaling using the B cell system as a model. Although most TLRs as well as IL-1R share MyD88 as an adaptor for triggering intracellular signaling, several other adaptor molecules such as TRIF contribute to the TLR signaling pathways[3]. Responses to TLR3, TLR4 and TLR9 ligands were considerably impaired in TAK1-defeicient B cells. Moreover, activation of MAPKs and NF-κB in response to TLR4 and TLR9 ligand was consistently impaired, although the activation was not completely abrogated even in the absence of TAK1. As TLR9 signaling depends completely on MyD88, it is obvious that TAK1 is important for MyD88-dependent signaling pathways. TLR4 activates MyD88-dependent and TRIF-dependent pathways. Both signaling pathways can activate NF-κB and MAPKs, although the time course differs. The MyD88-dependent pathway governs early activation of these signaling molecules, whereas the TRIF-dependent pathway is responsible for sustaining the activation[27,28]. In B cells, both MyD88 and TRIF are required for TLR4-induced proliferative response. In TLR4 signaling, the activation of NF-κB and MAPKs was considerably

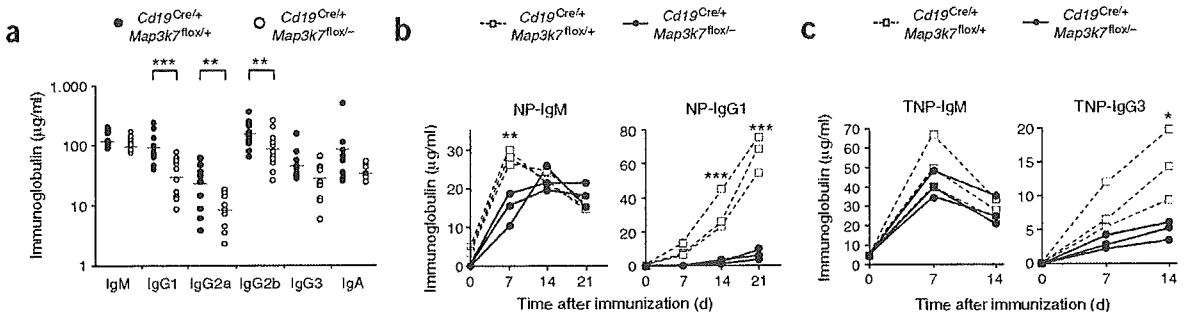

Figure 7 Impaired immune responses in *Cd19*$^{Cre/+}$*Map3k7*$^{flox/}$ mice. (**a**) Reduced basal immunoglobulin titers in *Cd19*$^{Cre/+}$*Map3k7*$^{flox/}$ mice. Immunoglobulin isotypes were measured by ELISA in the sera of nonimmunized 8-week-old *Cd19*$^{Cre/+}$*Map3k7*$^{flox/+}$ mice ($n = 12$) or *Cd19*$^{Cre/+}$*Map3k7*$^{flox/}$ mice ($n = 12$). Results are from individual mice. (**b**) Impaired T cell–dependent antibody responses in *Cd19*$^{Cre/+}$*Map3k7*$^{flox/}$ mice. Mice were immunized with nitrophenol–chicken γ-globulin, and nitrophenol (NP)–specific IgM and IgG1 production was measured by ELISA 7, 14 and 21 d after immunization. Results are from three (of five) representative mice per genotype. (**c**) Impaired T cell–independent type II antibody responses in *Cd19*$^{Cre/+}$*Map3k7*$^{flox/}$ mice. Mice were immunized with trinitrophenol-Ficoll, and trinitrophenol (TNP)–specific IgM and IgG3 production was measured 7 and 14 d after immunization. Results are from three (of five) representative mice per genotype. *, $P < 0.05$; **, $P < 0.01$ and ***, $P < 0.005$, versus TAK1-deficient cells (Student's *t*-test).

impaired in TAK1-deficient B cells at all time points examined, suggesting that MyD88-dependent and TRIF-dependent activation of these molecules depends entirely on TAK1.

Notably, TAK1 is also critical for B cell proliferation as well as Jnk activation in response to BCR crosslinking. Nevertheless, the activation of NF-κB and induction of NF-κB target genes induced by BCR-crosslinking was not impaired in TAK1-deficient B cells. In BCR signaling, a complex of CARD11, Bcl10 and MALT1 transduces signals to NF-κB and MAPKs downstream of protein kinase C-β[22]. CARD11 recruits Bcl10 to lipid rafts after stimulation. Bcl10 targets NF-κB essential modulator for K63-linked polyubiquitination through Ubc13 and MALT1 and activates NF-κB[29]. B cells from *Card11*$^{-/-}$, *Bcl10*$^{-/-}$ or *Malt1*$^{-/-}$ mice are reported to have defects in BCR signaling[30–36]. CARD11 is required for the activation of both NF-κB and Jnk[32]. Furthermore, *Bcl10*$^{-/-}$ B cells fail to activate NF-κB in response to BCR crosslinking. In contrast, B cells deficient in MALT1 (paracaspase) show impaired activation of NF-κB but not Jnk[34], indicating that Jnk is activated in a CARD11- and Bcl10-dependent, MALT1-independent signaling pathway. Given that TAK1 phosphorylates IKKs and MKK6 in IL-1β signaling, it is plausible that TAK1 is activated downstream of the CARD11-Bcl10-MALT1 complex and phosphorylates MAPKKs. In fact, we found that TAK1 interacted with Bcl10 in response to BCR crosslinking, indicating that TAK1 is recruited to the Bcl10 complex after BCR stimulation to induce Jnk activation. Although published work has shown that RNA interference–mediated knockdown of TAK1 in Jurkat cells results in diminished NF-κB activation in TCR signaling[23], our study has demonstrated that TAK1 is dispensable for NF-κB activation, at least in BCR signaling. That earlier report also showed that TRAF6 functions downstream of Bcl10 and MALT1 to activate NF-κB in TCR signaling[23]. Given that TAK1 interacts with Bcl10 in response to BCR but not LPS stimulation, it is likely that TAK1 is activated by Bcl10 without the intervention of TRAF6 in BCR signaling. As TAK1 is required for the activation of Jnk but not NF-κB, MALT1-mediated activation of the IKK complex probably occurs independently of TAK1. These results collectively indicate that in B cells, CARD11 and Bcl10 might activate TAK1 and MALT1 to regulate MAPKKs and IKKs, respectively.

Although TAK1-deficient B cells failed to proliferate in response to BCR crosslinking, activation of NF-κB was not impaired. Consistent with that finding, the upregulation of cyclin D2 was not altered in TAK1-deficient B cells. However, downregulation of p27^{Kip1} was impaired in TAK1-deficient B cells, suggesting that TAK1-dependent signaling might regulate G1-S progression at the level of p27^{Kip1} degradation. So far, it is not clear whether Jnk alone is responsible for the defect in the proliferation in TAK1-deficient B cells. It is possible that TAK1 regulates the activation of as-yet-unknown signaling pathway(s) in addition to Jnk and that the pathways cooperatively control BCR-mediated proliferation. Additional studies are needed to clarify the molecular mechanisms of cell cycle progression in BCR signaling.

Involvement of TAK1 in early embryogenesis modifying bone morphogenic protein signaling has been suggested[37]. *Map3k7*$^{-/-}$ embryos died at E9.5–E10.5. Mice deficient in genes encoding molecules involved in NF-κB signaling, such as RelA (also called p65) and IKKβ, die *in utero* due to massive liver apoptosis[38–41]. However, *Map3k7*$^{-/-}$ mice die before the initiation of fetal liver development, suggesting that the function of TAK1 in embryonic development is not explained by NF-κB inhibition. TAB1-deficient mice die between E15.5 and E18.5 due to edema and hemorrhage, and TAB2-deficient mice die between E11.5 and E12.5 due to liver apoptosis[18,19]. Thus, the function of TAK1 in embryogenesis might be independent of TAB1 or TAB2. The TAK1-NLK-STAT3 cascade is essential for TGF-β-mediated mesoderm formation in xenopus embryos[42]. Additional studies will be needed to clarify the mechanisms of the involvement of TAK1 in early embryogenesis.

In conclusion, we have shown here that TAK1 is essential for MAPK and NF-κB activation in response to TLR, IL-1R and TNFR stimulation. Consistent with those findings, TAK1-deficient cells failed to activate in response to TLR ligands, IL-1β and TNF. Antigen-induced B cell proliferation as well as immune responses to experimental antigens were considerably impaired in mice with B cell–specific TAK1-deficiency, indicating that TAK1 is involved in both innate and adaptive immunity. These data provide genetic evidence that TAK1 kinase has nonredundant functions in signaling pathways in inflammatory and immune responses.

METHODS

Generation of *Map3k7* mutant mice. Phage clones containing mouse *Map3k7* were isolated by screening of a 129/SvJ genomic library (Stratagene) with a probe corresponding to the 5′ end of mouse TAK1 cDNA. A targeting vector was designed to flank exon 2, containing the sequence encoding the ATP-binding site, with two *lox*P sites. The floxed neomycin-resistance gene fragment was inserted into intron 1 of *Map3k7*. A 1.0-kilobase (kb) *Cla*I–*Bam*HI

© 2005 Nature Publishing Group http://www.nature.com/natureimmunology

fragment was used as the 5′ homology region; a 2.5-kb *Xba*I–*Sal*I fragment, which contains exon 2 of *Map3k7*, was inserted between the two *lox*P sites; and a 6.0-kb *Not*I–*Sac*II fragment was used as the 3′ homology region. The herpes simplex virus thymidine kinase gene was used for negative selection of clones with random integration. A total of 30 μg of *Sac*II-linearized vector was electroporated into E14.1 embryonic stem cells. After positive and negative selection with G418 and ganciclovir, drug-resistant clones were picked up and were screened by PCR and Southern blot analysis. These clones were individually microinjected into blastocysts derived from C57BL/6 mice and were transferred to pseudopregnant females. Matings of chimeric male mice to C57BL/6 female mice resulted in transmission of the floxed allele to the germline. *Map3k7*$^{flox/+}$ or *Map3k7*$^{flox/flox}$ mice were bred with transgenic mouse line carrying the *Cre* transgene under control of the cytomegalovirus immediate early enhancer–chicken β-actin hybrid (*CAG*) promoter[43] to generate the *CAG*$^{Cre/+}$*Map3k7*$^{flox/+}$ (genotype, *Map3k7*$^{+/}$), which were then intercrossed to generate *CAG*$^{Cre/+}$*Map3k7*$^{flox/flox}$ (genotype, *Map3k7* $^{/}$) mice. All animal experiments were done with the approval of the Animal Research Committee of the Research Institute for Microbial Diseases (Osaka University, Osaka, Japan).

Establishment of *Map3k7* $^{/}$ MEFs. MEFs were obtained from E13.5 *Map3k7*$^{flox/flox}$ embryos, were immortalized according to a general 3T3 protocol[44] and were cloned. For excision of the floxed genomic fragment containing exon 2, two different clones of *Map3k7*$^{flox/flox}$ MEFs were infected with retrovirus expressing Cre protein together with GFP or were infected with GFP alone (to establish control MEFs). GFP^{+} cells were sorted by FACSVantage (Becton Dickinson) and then were analyzed by Southern blot and immunoblot to confirm genotype.

Generation of mice with B cell–specific TAK1 deficiency. Mice carrying the *Cre* transgene under control of the *Cd19* promoter[45] were bred with *Map3k7*$^{+/}$ mice to generate *Cd19*$^{Cre/+}$*Map3k7*$^{+/}$ mice. These mice were mated with *Map3k7*$^{flox/flox}$ mice; *Cd19*$^{Cre/+}$*Map3k7*$^{flox/+}$ or *Cd19*$^{Cre/+}$*Map3k7*$^{flox/}$ offspring were used for analysis.

Purification of B cells. Resting B cells were isolated from single-cell suspensions of spleen cells by depletion of CD43^{+} cells with anti-CD43 magnetic beads (MACS; Miltenyi Biotec). Cell purity was typically more than 95% B220^{+}, as assessed by flow cytometry.

Immunoblot analysis. Cells were lysed in a lysis buffer containing 1.0% Nonidet-P40, 150 mM NaCl, 20 mM Tris-HCl, pH 7.5, 1 mM EDTA and a protease inhibitor 'cocktail' (Roche). Lysates were separated by SDS-PAGE and were transferred onto polyvinylidene difluoride membranes (BioRad). After membranes were blotted with antibodies, proteins on membranes were visualized with an enhanced chemiluminescence system (Perkin-Elmer). Polyclonal anti-TAK1, anti-TAB1, anti-TAB2 and anti-IRAK-1 were as described[8,15,46]. Polyclonal antibody to phosphorylated Jnk (anti-phospho-Jnk), anti-phospho-p38, anti-phospho-Erk and anti-phospho-IκBα were purchased from Cell Signaling. Polyclonal anti-Jnk, anti-p38, anti-Erk, anti-IκBα, anti-p27^{Kip1} and anti–cyclin D2 and monoclonal anti-Bcl10 (clone 331.3) were from Santa Cruz. Monoclonal anti-phosphotyrosine (clone 4G10) was purchased from Upstate Biotechnology. Polyclonal anti-CARD11 was from Alexis Biochemicals.

Luciferase reporter assay. HEK293 cells were transiently transfected with 100 ng of either NF-κB (5) or AP-1 luciferase reporter plasmids, together with a total of 1.0 μg expression vector(s). Then, 48 h later, the luciferase activity in the total cell lysate was measured with the Dual-luciferase reporter assay system (Promega).

Measurement of IL-6 production. MEFs (2 10^{4}) and purified splenic B cells (5 10^{4}) were stimulated for 48 h with recombinant mouse IL-1β (R&D Systems) and LPS (Sigma) or with CpG DNA (ODN1668; Hokkaido System Science), respectively. Culture supernatants were collected and IL-6 was measured with an ELISA kit (R&D Systems).

Cell viability. MEFs (2 10^{5}) were seeded onto six-well plates and were treated for 24 h with various concentrations of recombinant mouse TNF (R&D Systems). Purified splenic B cells (1 10^{6}) were stimulated with LPS, CpG DNA or anti-IgM (Jackson ImmunoResearch) for various periods. Cell viability was assessed with annexin V–indocarbocyanine (BioVision) and a FACSCalibur (Becton Dickinson).

Electrophoretic mobility-shift assay (EMSA). MEFs (1 10^{6}) or purified splenic B cells (5 10^{6}) were treated with stimuli for various periods. Nuclear extracts were purified from cells, were incubated with a probe specific for the NF-κB DNA-binding site, were separated by electrophoresis and were visualized by autoradiography as described[47].

Flow cytometry. Single-cell suspensions were prepared from thymi, bone marrow, spleens and peritoneal cavities of untreated mice. Cells were stained with fluorescein isothiocyanate–, phycoerythrin- or allophycocyanin-conjugated antibodies (Pharmingen) and then were analyzed on a FACSCalibur.

***In vivo* immunization and ELISA.** Mice were immunized intraperitoneally with 50 μg nitrophenol–chicken γ-globulin (Biosearch Technologies) precipitated with Imject alum (Pierce) or with 25 μg trinitrophenol-Ficoll (Biosearch Technologies). Antigen- and isotype-specific antibodies were measured by ELISA in sera collected from peripheral blood at various time points, on plates coated with nitrophenol-BSA or trinitrophenol-BSA. Antibodies to mouse IgM, IgG1, IgG2a, IgG2b, IgG3 and IgA were purchased from Southern Biotechnology.

B cell proliferation assay. Purified splenic B cells (5 10^{4}) were cultured in 96-well plates for 48 h with various concentrations of LPS, CpG DNA, poly(I:C) (Amersham), anti-IgM or anti-CD40 (Pharmingen). Samples were pulsed with 1 μCi [^{3}H]thymidine for the last 12 h and then ^{3}H uptake was measured with a β-scintillation counter (Packard).

Cell cycle analysis. Cell cycles of B cells were analyzed with the BrdU Flow Kit (Pharmingen) according to the manufacturer's instructions. Cells were cultured with LPS, CpG DNA or anti-IgM for 24 h, were pulsed with 10 μM BrdU for an additional 16 h, were stained with fluorescein isothiocyanate–anti-BrdU and 7-amino-actinomycin D and then were analyzed by flow cytometry.

Microarray analysis. Purified splenic B cells were treated for 4 h with or without anti-IgM (20 μg/ml). Total RNA was extracted with an RNeasy kit (Qiagen), and double-stranded DNA was synthesized from 10 μg of total RNA with the SuperScript Choice System (Invitrogen) primed with a T7-Oligo primer (Affymetrix). This cDNA was used to prepare biotin-labeled cRNA by an *in vitro* transcription reaction done with T7 RNA polymerase in the presence of biotinylated ribonucleotides, according to the manufacturer's protocol (Enzo Diagnostics). The cRNA product was purified with an RNeasy kit and fragmented and was hybridized to Affymetrix mouse expression array A430.2 microarray chips according to the manufacturer's protocol (Affymetrix). The hybridized chips were stained and washed and were scanned with a GeneArray Scanner (Affymetrix).

Accession code. GEO: microarray data, GSE3065.

Note: Supplementary information is available on the Nature Immunology website.

ACKNOWLEDGMENTS

We thank R.C. Rickert (The Burnham Institute, La Jolla, California) for providing *Cd19-Cre* mice; J. Miyazaki (Osaka University, Suita, Japan) for providing *CAG-Cre* mice; T. Kitamura (University of Tokyo, Tokyo, Japan) for providing retrovirus vector; D.T. Golenbock (University of Massachusetts Medical School, Worcester, Massachusetts) for providing NF-κB reporter; T. Kaisho and Y. Kumagai for discussions; K. Nakamura for cell sorting; A. Shibano, M. Shiokawa, Y. Fujiwara and N. Kitagaki for technical assistance; and M. Hashimoto and E. Horita for secretarial assistance. Supported by Special Coordination Funds, the Ministry of Education, Culture, Sports, Science and Technology.

COMPETING INTERESTS STATEMENT

The authors declare that they have no competing financial interests.

Published online at http://www.nature.com/natureimmunology/
Reprints and permissions information is available online at http://npg.nature.com/reprintsandpermissions/

1. Aggarwal, B.B. Signalling pathways of the TNF superfamily: a double-edged sword. *Nat. Rev. Immunol.* **3**, 745–756 (2003).

© 2005 Nature Publishing Group http://www.nature.com/natureimmunology

2. Dinarello, C.A. Biologic basis for interleukin-1 in disease. *Blood* **87**, 2095–2147 (1996).
3. Akira, S. & Takeda, K. Toll-like receptor signalling. *Nat. Rev. Immunol.* **4**, 499–511 (2004).
4. Baud, V. & Karin, M. Signal transduction by tumor necrosis factor and its relatives. *Trends Cell Biol.* **11**, 372–377 (2001).
5. Deng, L. *et al.* Activation of the IκB kinase complex by TRAF6 requires a dimeric ubiquitin-conjugating enzyme complex and a unique polyubiquitin chain. *Cell* **103**, 351–361 (2000).
6. Wang, C. *et al.* TAK1 is a ubiquitin-dependent kinase of MKK and IKK. *Nature* **412**, 346–351 (2001).
7. Ghosh, S. & Karin, M. Missing pieces in the NF-κB puzzle. *Cell* **109**, S81–S96 (2002).
8. Ninomiya-Tsuji, J. *et al.* The kinase TAK1 can activate the NIK-IκB as well as the MAP kinase cascade in the IL-1 signalling pathway. *Nature* **398**, 252–256 (1999).
9. Yamaguchi, K. *et al.* Identification of a member of the MAPKKK family as a potential mediator of TGF-β signal transduction. *Science* **270**, 2008–2011 (1995).
10. Vidal, S. *et al.* Mutations in the *Drosophila* dTAK1 gene reveal a conserved function for MAPKKKs in the control of rel/NF-κB-dependent innate immune responses. *Genes Dev.* **15**, 1900–1912 (2001).
11. Takaesu, G. *et al.* TAK1 is critical for IκB kinase-mediated activation of the NF-κB pathway. *J. Mol. Biol.* **326**, 105–115 (2003).
12. Irie, T., Muta, T. & Takeshige, K. TAK1 mediates an activation signal from toll-like receptor(s) to nuclear factor-κB in lipopolysaccharide-stimulated macrophages. *FEBS Lett.* **467**, 160–164 (2000).
13. Wan, J. *et al.* Elucidation of the c-Jun N-terminal kinase pathway mediated by Estein-Barr virus-encoded latent membrane protein 1. *Mol. Cell. Biol.* **24**, 192–199 (2004).
14. Shibuya, H. *et al.* TAB1: an activator of the TAK1 MAPKKK in TGF-β signal transduction. *Science* **272**, 1179–1182 (1996).
15. Takaesu, G. *et al.* TAB2, a novel adaptor protein, mediates activation of TAK1 MAPKKK by linking TAK1 to TRAF6 in the IL-1 signal transduction pathway. *Mol. Cell* **5**, 649–658 (2000).
16. Ishitani, T. *et al.* Role of the TAB2-related protein TAB3 in IL-1 and TNF signaling. *EMBO J.* **22**, 6277–6288 (2003).
17. Cheung, P.C., Nebreda, A.R. & Cohen, P. TAB3, a new binding partner of the protein kinase TAK1. *Biochem. J.* **378**, 27–34 (2004).
18. Sanjo, H. *et al.* TAB2 is essential for prevention of apoptosis in fetal liver but not for interleukin-1 signaling. *Mol. Cell. Biol.* **23**, 1231–1238 (2003).
19. Komatsu, Y. *et al.* Targeted disruption of the Tab1 gene causes embryonic lethality and defects in cardiovascular and lung morphogenesis. *Mech. Dev.* **119**, 239–249 (2002).
20. Wagner, M. *et al.* IL-12p70-dependent Th1 induction by human B cells requires combined activation with CD40 ligand and CpG DNA. *J. Immunol.* **172**, 954–963 (2004).
21. Kurosaki, T. Regulation of B-cell signal transduction by adaptor proteins. *Nat. Rev. Immunol.* **2**, 354–363 (2002).
22. Thome, M. CARMA1, BCL-10 and MALT1 in lymphocyte development and activation. *Nat. Rev. Immunol.* **4**, 348–359 (2004).
23. Sun, L., Deng, L., Ea, C.K., Xia, Z.P. & Chen, Z.J. The TRAF6 ubiquitin ligase and TAK1 kinase mediate IKK activation by BCL10 and MALT1 in T lymphocytes. *Mol. Cell* **14**, 289–301 (2004).
24. Sidorova, E.V., Li-Sheng, L., Devlin, B., Chernishova, I. & Gavrilova, M. Role of different B-cell subsets in the specific and polyclonal immune response to T-independent antigens type 2. *Immunol. Lett.* **88**, 37–42 (2003).
25. Jin, G. *et al.* Identification of a human NF-κB-activating protein, TAB3. *Proc. Natl. Acad. Sci. USA* **101**, 2028–2033 (2004).
26. Kanayama, A. *et al.* TAB2 and TAB3 activate the NF-κB pathway through binding to polyubiquitin chains. *Mol. Cell* **15**, 535–548 (2004).
27. Kawai, T., Adachi, O., Ogawa, T., Takeda, K. & Akira, S. Unresponsiveness of MyD88-deficient mice to endotoxin. *Immunity* **11**, 115–122 (1999).
28. Yamamoto, M. *et al.* Role of adaptor TRIF in the MyD88-independent toll-like receptor signaling pathway. *Science* **301**, 640–643 (2003).
29. Zhou, H. *et al.* Bcl10 activates the NF-κB pathway through ubiquitination of NEMO. *Nature* **427**, 167–171 (2004).
30. Ruland, J. *et al.* Bcl10 is a positive regulator of antigen receptor-induced activation of NF-κB and neural tube closure. *Cell* **104**, 33–42 (2001).
31. Egawa, T. *et al.* Requirement for CARMA1 in antigen receptor-induced NF-κB activation and lymphocyte proliferation. *Curr. Biol.* **13**, 1252–1258 (2003).
32. Hara, H. *et al.* The MAGUK family protein CARD11 is essential for lymphocyte activation. *Immunity* **18**, 763–775 (2003).
33. Newton, K. & Dixit, V.M. Mice lacking the CARD of CARMA1 exhibit defective B lymphocyte development and impaired proliferation of their B and T lymphocytes. *Curr. Biol.* **13**, 1247–1251 (2003).
34. Ruefli-Brasse, A.A., French, D.M. & Dixit, V.M. Regulation of NF-κB-dependent lymphocyte activation and development by paracaspase. *Science* **302**, 1581–1584 (2003).
35. Ruland, J., Duncan, G.S., Wakeham, A. & Mak, T.W. Differential requirement for Malt1 in T and B cell antigen receptor signaling. *Immunity* **19**, 749–758 (2003).
36. Xue, L. *et al.* Defective development and function of Bcl10-deficient follicular, marginal zone and B1 B cells. *Nat. Immunol.* **4**, 857–865 (2003).
37. Munoz-Sanjuan, I., Bell, E., Altmann, C.R., Vonica, A. & Brivanlou, A.H. Gene profiling during neural induction in *Xenopus laevis*: regulation of BMP signaling by post-transcriptional mechanisms and TAB3, a novel TAK1-binding protein. *Development* **129**, 5529–5540 (2002).
38. Beg, A.A., Sha, W.C., Bronson, R.T., Ghosh, S. & Baltimore, D. Embryonic lethality and liver degeneration in mice lacking the RelA component of NF-κB. *Nature* **376**, 167–170 (1995).
39. Tanaka, M. *et al.* Embryonic lethality, liver degeneration, and impaired NF-κB activation in IKK-β-deficient mice. *Immunity* **10**, 421–429 (1999).
40. Li, Q., Van Antwerp, D., Mercurio, F., Lee, K.F. & Verma, I.M. Severe liver degeneration in mice lacking the IκB kinase 2 gene. *Science* **284**, 321–325 (1999).
41. Rudolph, D. *et al.* Severe liver degeneration and lack of NF-κB activation in NEMO/IKKγ-deficient mice. *Genes Dev.* **14**, 854–862 (2000).
42. Ohkawara, B. *et al.* Role of the TAK1-NLK-STAT3 pathway in TGF-β-mediated mesoderm induction. *Genes Dev.* **18**, 381–386 (2004).
43. Sakai, K., Mitani, K. & Miyazaki, J. Efficient regulation of gene expression by adenovirus vector-mediated delivery of the CRE recombinase. *Biochem. Biophys. Res. Commun.* **217**, 393–401 (1995).
44. Todaro, G.J. & Green, H. Quantitative studies of the growth of mouse embryo cells in culture and their development into established lines. *J. Cell Biol.* **17**, 299–313 (1963).
45. Rickert, R.C., Roes, J. & Rajewsky, K. B lymphocyte-specific, Cre-mediated mutagenesis in mice. *Nucleic Acids Res.* **25**, 1317–1318 (1997).
46. Sato, S. *et al.* A variety of microbial components induce tolerance to lipopolysaccharide by differentially affecting MyD88-dependent and -independent pathways. *Int. Immunol.* **14**, 783–791 (2002).
47. Sato, S. *et al.* Synergy and cross-tolerance between toll-like receptor (TLR) 2- and TLR4-mediated signaling pathways. *J. Immunol.* **165**, 7096–7101 (2000).

© 2005 Nature Publishing Group http://www.nature.com/natureimmunology

Immunity 24, 41–51, January 2006 ©2006 Elsevier Inc. DOI 10.1016/j.immuni.2005.11.004

IκBNS Inhibits Induction of a Subset of Toll-like Receptor-Dependent Genes and Limits Inflammation

Hirotaka Kuwata,[1] Makoto Matsumoto,[1] Koji Atarashi,[1] Hideaki Morishita,[1] Tomohiro Hirotani,[2] Ritsuko Koga,[1] and Kiyoshi Takeda[1,*]
[1] Department of Molecular Genetics
Medical Institute of Bioregulation
Kyushu University
3-1-1 Maidashi, Higashi-ku
Fukuoka 812-8582
Japan
[2] Department of Gastroenterology and Hepatology
Graduate School of Medicine
Osaka University
2-2 Yamada-oka, Suita
Osaka 565-0871
Japan

Summary

Toll-like receptor (TLR)-mediated immune responses are downregulated by several mechanisms that affect signaling pathways. However, it remains elusive how TLR-mediated gene expression is differentially modulated. Here, we show that IκBNS, a TLR-inducible nuclear IκB protein, negatively regulates induction of a subset of TLR-dependent genes through inhibition of NF-κB activity. IκBNS-deficient macrophages and dendritic cells show increased TLR-mediated expression of genes such as IL-6 and IL-12p40, which are induced late after TLR stimulation. In contrast, IκBNS-deficient cells showed normal induction of genes that are induced early or induced via IRF-3 activation. LPS stimulation of IκBNS-deficient macrophages prolonged NF-κB activity at the specific promoters, indicating that IκBNS mediates termination of NF-κB activity at selective gene promoters. Moreover, IκBNS-deficient mice are highly susceptible to LPS-induced endotoxin shock and intestinal inflammation. Thus, IκBNS regulates inflammatory responses by inhibiting the induction of a subset of TLR-dependent genes through modulation of NF-κB activity.

Introduction

Toll-like receptors (TLRs) are implicated in the recognition of specific patterns of microbial components and subsequent induction of gene expression. TLR-dependent gene expression is induced through activation of two distinct signaling pathways mediated by the Toll/IL-1 receptor (TIR) domain-containing adaptors MyD88 and TRIF. These signaling pathways finally culminate in the activation of several transcription factors, such as NF-κB and IRF families (Akira and Takeda, 2004). The MyD88-dependent gene induction is achieved by an early phase of NF-κB and IRF-5 activation in macrophages (Kawai et al., 1999; Takaoka et al., 2005). The TRIF-dependent gene induction is mainly regulated by IRF-3 (Sakaguchi et al., 2003; Yamamoto et al., 2003).

TLR-mediated gene expression regulates activation of not only innate immunity but also adaptive immunity, which provides antigen-specific responses against harmful pathogens (Iwasaki and Medzhitov, 2004; Pasare and Medzhitov, 2004). However, TLR-mediated activation of innate immunity, when in excess, triggers development of autoimmune disorders and inflammatory diseases, such as SLE, cardiomyopathy, atherosclerosis, diabetes mellitus, and inflammatory bowel diseases (Bjorkbacka et al., 2004; Eriksson et al., 2003; Kobayashi et al., 2003; Lang et al., 2005; Leadbetter et al., 2002; Michelsen et al., 2004). Excessive activation of TLR4 by LPS induces endotoxin shock, a serious systemic disorder with a high mortality rate. Therefore, TLR-dependent innate immune responses must be finely regulated, and underlying mechanisms are now being examined extensively (Liew et al., 2005). Several negative regulators of TLR-mediated signaling pathways have been proposed. Cytoplasmic molecules, such as an alternatively spliced short form of MyD88 (MyD88s), IRAK-M, SOCS1, A20, PI3-kinase, and TRIAD3A, are all involved in negative regulation of TLR pathways (Boone et al., 2004; Burns et al., 2003; Chuang and Ulevitch, 2004; Fukao et al., 2002; Kinjyo et al., 2002; Kobayashi et al., 2002; Nakagawa et al., 2002). Membrane bound SIGIRR, ST2, TRAILR, and RP105 are also implicated in these processes (Brint et al., 2004; Diehl et al., 2004; Divanovic et al., 2005; Wald et al., 2003).

TLR-dependent gene induction is also regulated by nuclear IκB proteins, such as IκBζ, Bcl-3, and IκBNS. IκBζ is indispensable for positive regulation of a subset of TLR-dependent genes, such as IL-6 and IL-12p40 (Yamamoto et al., 2004). In contrast, Bcl-3 and IκBNS seem to be involved in negative regulation of TLR-dependent gene induction. Bcl-3 was shown to be involved in selective inhibition of TLR-dependent TNF-α production (Kuwata et al., 2003; Wessells et al., 2004). An in vitro study indicated that IκBNS is induced by IL-10 or LPS and selectively inhibits IL-6 production in macrophages (Hirotani et al., 2005). Thus, nuclear IκB proteins differentially regulate TLR-dependent gene expression. However, the physiological role of IκBNS is still unclear.

In this study, we analyzed TLR-dependent inflammatory responses in IκBNS-deficient mice. We found that IκBNS is involved in selective inhibition of a subset of MyD88-dependent genes, including IL-6, IL-12p40, and IL-18. In IκBNS-deficient macrophages, LPS-induced activation of NF-κB was prolonged. Accordingly, IκBNS-deficient mice showed increased production of these cytokines accompanied by high sensitivity to LPS-induced endotoxin shock. Furthermore, IκBNS-deficient mice were highly susceptible to intestinal inflammation caused by disruption of the epithelial barrier. These findings indicate that IκBNS inhibits the induction of a group of TLR-dependent genes, thereby preventing excessive inflammation.

*Correspondence: ktakeda@bioreg.kyushu-u.ac.jp

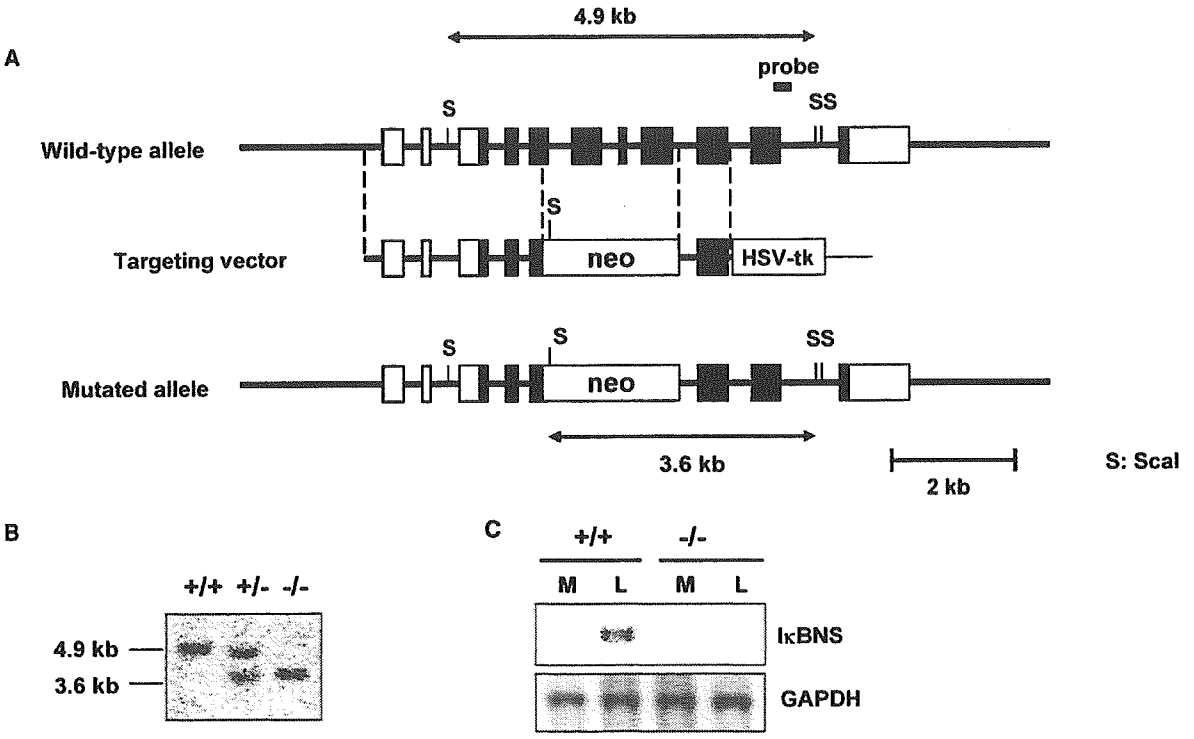

Figure 1. Targeted Disruption of the Mouse *Ikbns* Gene

(A) Maps of the IκBNS wild-type genome, targeting vector, and predicted targeted gene. Open and closed boxes denote the noncoding and coding exons, respectively. Restriction enzymes: S, ScaI.

(B) Southern blot analysis of offspring from the heterozygote intercrosses. Genomic DNA was extracted from mouse tails, digested with ScaI, electrophoresed, and hybridized with the probe indicated in (A). The approximate size of the wild-type band is 4.9 kb, and the mutated band is 3.6 kb.

(C) Peritoneal macrophages were cultured with or without 100 ng/ml LPS for 1 hr (L and M, respectively), and total RNA was extracted, electrophoresed, transferred to nylon membrane, and hybridized with the mouse IκBNS full-length cDNA probe. The same membrane was rehybridized with a GAPDH probe.

Results

Targeted Disruption of the IκBNS Gene

To study the functional role of IκBNS in TLR-dependent responses, a null mutation in the *Ikbns* allele was introduced through homologous recombination in embryonic stem (ES) cells (Figures 1A and 1B). IκBNS$^{-/-}$ mice were born alive and grew healthy until 20 weeks of age. We performed Northern blot analysis to confirm that the mutation causes inactivation of the *Ikbns* gene. LPS robustly induced IκBNS mRNA in wild-type macrophages, but not in IκBNS$^{-/-}$ macrophages (Figure 1C).

A previous report indicated that IκBNS is involved in negative selection of thymocytes (Fiorini et al., 2002). Therefore, we first analyzed lymphocyte composition in lymphoid organs such as thymus and spleen by flow cytometry (Figures S1A and S1B). Total cell number and CD4/CD8 or CD3/B220 populations in thymus and spleen were not altered in IκBNS$^{-/-}$ mice. Splenic T cells from IκBNS$^{-/-}$ mice showed similar levels of proliferative responses to IL-2 and IL-7 as did wild-type T cells. Moreover, IκBNS$^{-/-}$ T cells proliferated to almost equal degrees in response to anti-CD3 antibody compared to wild-type T cells (Figure S1C). These results indicate that T cell development and functions were generally unaffected in IκBNS$^{-/-}$ mice.

Increased IL-6 and IL-12p40 Production in IκBNS-Deficient Cells

Since IκBNS expression was induced within 1 hr of LPS stimulation in macrophages (Figure 1B), we stimulated peritoneal macrophages with various concentrations of LPS and analyzed for production of TNF-α and IL-6 (Figure 2A). In macrophages from IκBNS$^{-/-}$ mice, LPS-induced TNF-α production was comparable to wild-type cells, but IL-6 production was significantly increased. We then analyzed whether IκBNS$^{-/-}$ macrophages produce increased amounts of IL-6 in response to other TLR ligands, since IκBNS mRNA was induced by several TLR ligands as well as the TLR4 ligand LPS in a MyD88-dependent manner (Figure S2A). Peritoneal macrophages were stimulated with mycoplasmal lipopeptides (TLR6 ligand), Pam_3CSK_4 (TLR1 ligand), peptidoglycan (TLR2 ligand), and imiquimod (TLR7 ligand), and analyzed for production of TNF-α and IL-6 (Figure 2B). In response to these TLR ligands, the production of IL-6, but not TNF-α, was increased in IκBNS$^{-/-}$ mice. We next analyzed the response of bone marrow-derived dendritic cells (DCs). DCs from IκBNS$^{-/-}$ mice produced similar amounts of TNF-α and increased amounts of IL-6 in response to LPS compared to wild-type DCs (Figure 2C). In addition, DCs showed LPS-induced production of IL-12p40 and IL-12p70, and production of these

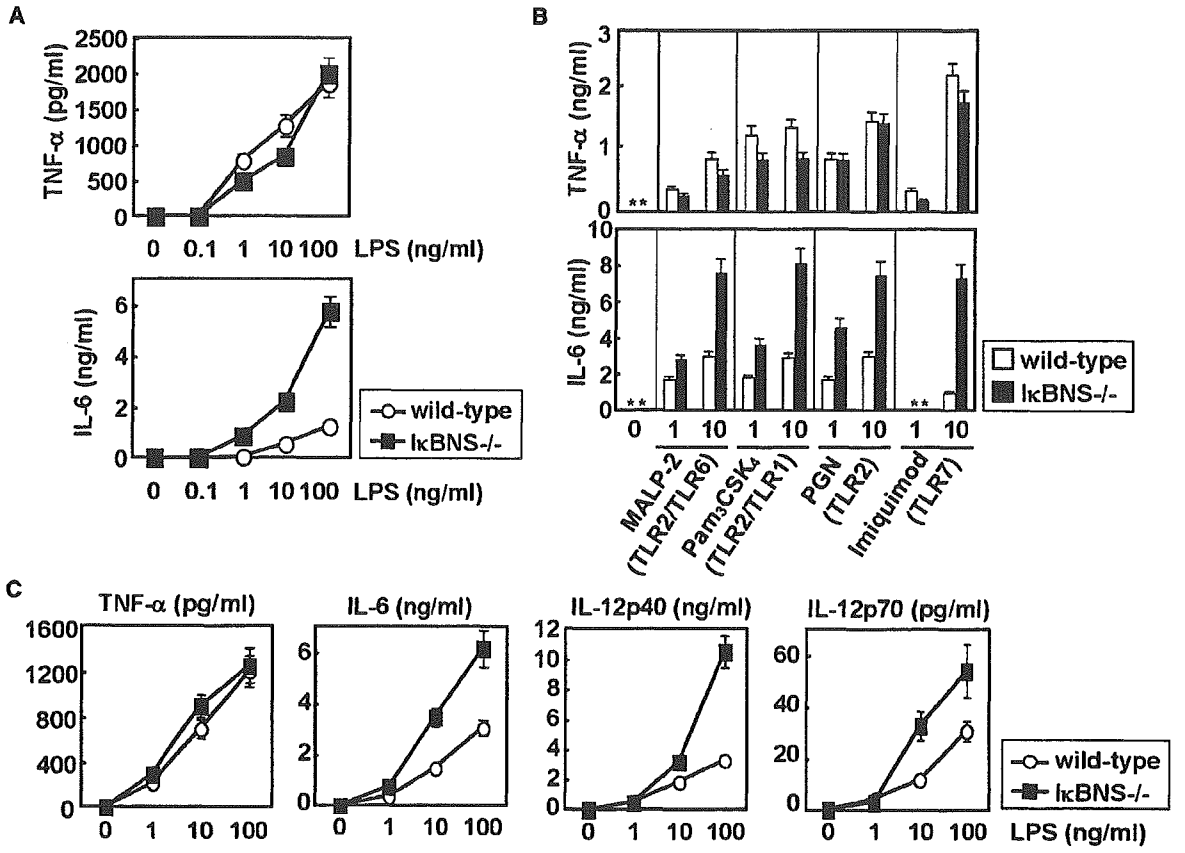

Figure 2. Increased Production of IL-6 and IL-12p40 in IκBNS$^{-/-}$ Macrophages and Dendritic Cells

(A) Peritoneal macrophages were stimulated with the indicated concentration of LPS for 24 hr. Concentrations of TNF-α and IL-6 in the culture supernantants were analyzed by ELISA. Data are mean ± SD of triplicate cultures in a single experiment, representative of three independent experiments.

(B) Peritoneal macrophages were cultured with 1 or 10 ng/ml of TLR6 ligand (MALP-2), 1 or 10 ng/ml TLR1 ligand (Pam_3CSK_4), 1 or 10 μg/ml TLR2 ligand (peptidoglycan; PGN), or 1 or 10 μg/ml TLR7 ligand (imiquimod) for 24 hr. Concentrations of TNF-α and IL-6 in the culture supernatants were analyzed by ELISA. *; not detected.

(C) Bone marrow-derived DCs were stimulated with the indicated concentration of LPS for 24 hr. Concentrations of TNF-α, IL-6, IL-12p40, and IL-12p70 in the culture supernatants were analyzed by ELISA. Data are mean ± SD of triplicate cultures in a single experiment, representative of three independent experiments.

cytokines was significantly increased in IκBNS$^{-/-}$ DCs. Bone marrow-derived DCs and splenic B cells were analyzed for LPS-induced surface expression of CD86 or MHC class II (Figure S2B). LPS-induced augmentation of surface expression of these molecules was not altered in IκBNS$^{-/-}$ mice. Thus, macrophages and DCs from IκBNS$^{-/-}$ mice showed selective increases in TLR-dependent production of IL-6 and IL-12p40.

Enhanced Induction of a Subset of TLR-Dependent Genes in IκBNS-Deficient Macrophages

We further analyzed LPS-induced mRNA expression of TLR-dependent genes in IκBNS$^{-/-}$ macrophages. Peritoneal macrophages were stimulated with LPS for 1, 3, or 5 hr, and total RNA was extracted. Then, mRNA expression of TNF-α and IL-6 was first analyzed by quantitative real-time RT-PCR (Figures 3A and 3B). LPS-induced TNF-α mRNA expression in IκBNS$^{-/-}$ macrophages was similar to wild-type cells. In the case of IL-6 mRNA, expression levels were comparable between wild-type and IκBNS$^{-/-}$ macrophages until 3 hr of LPS stimulation. After 3 hr, IL-6 mRNA levels decreased in wild-type cells. However, IκBNS$^{-/-}$ cells displayed further enhanced expression of IL-6 mRNA. TNF-α mRNA was robustly induced within 1 hr of LPS stimulation, and its expression promptly ceased in wild-type cells. In contrast, IL-6 mRNA expression was induced late compared to TNF-α. Because LPS-induced IκBNS mRNA expression showed similar patterns as TNF-α mRNA, we hypothesized that LPS-inducible IκBNS blocks mRNA expression of genes that are induced late (Figure 3C). Accordingly, we analyzed mRNA expression of other genes that are induced early (*Il-1β*, *Il-23p19*, or *Ikbz*) or late (*Il-12p40*, *Il-18*, or *Csf3*) in response to LPS. LPS-induced mRNA expression of *Il-1β* (IL-1β), *Il-23p19* (IL-23p19), and *Ikbz* (IκBζ) was similarly observed between wild-type and IκBNS$^{-/-}$ macrophages (Figure 3A). LPS-induced expression of *Il-12p40* (IL-12p40), *Il-18* (IL-18) and *Csf3* (G-CSF) was observed at normal levels in IκBNS$^{-/-}$ macrophages at the early phase of LPS stimulation (within 3 hr of LPS stimulation) (Figure 3B). However, at the late phase of LPS stimulation (after 3 hr of LPS stimulation), mRNA expression of these genes was significantly enhanced in

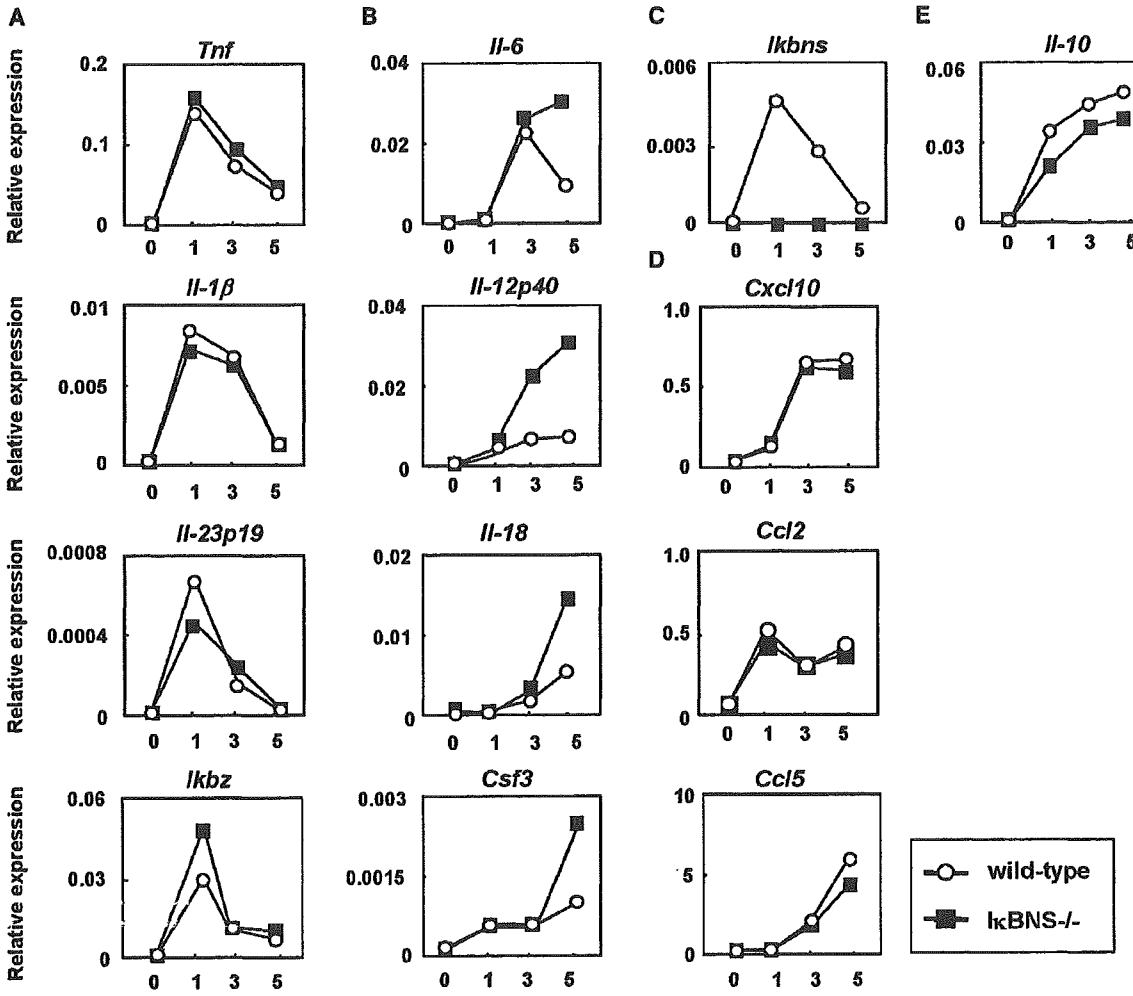

Figure 3. LPS-Induced Expression of Several TLR-Dependent Genes in IκBNS$^{-/-}$ Macrophages

Peritoneal macrophages from wild-type and IκBNS$^{-/-}$ mice were stimulated with 100 ng/ml LPS for the indicated periods. Total RNA was extracted, and then subjected to quantitative real-time RT-PCR analysis using primers specific for *Tnf*, *Il-1β*, *Il-23p19*, *Ikbz* (A), *Il-6*, *Il-12p40*, *Il-18*, *Csf3* (B), *Ikbns* (C), *Cxcl10*, *Ccl2*, *Ccl5* (D), and *Il-10* (E). The fold difference of each sample relative to EF-1α levels is shown. Representative of three independent experiments.

IκBNS$^{-/-}$ cells. We also analyzed LPS-induced expression of *Cxcl10* (IP-10), *Ccl2* (MCP-1), and *Ccl5* (RANTES), which are induced by the TRIF-dependent activation of IRF-3 (Figure 3D). LPS-induced expression of these genes was not altered in IκBNS$^{-/-}$ macrophages. An anti-inflammatory cytokine IL-10 is induced by TLR stimulation and thereby inhibits TLR-dependent gene induction (Moore et al., 2001). Therefore, we next addressed LPS-induced IL-10 mRNA expression (Figure 3E). LPS-induced IL-10 mRNA expression was comparable between wild-type and IκBNS$^{-/-}$ macrophages. In addition, LPS-induced production of IL-10 protein was not compromised in IκBNS$^{-/-}$ DCs (Figure S2C). These findings indicate that the enhanced LPS-induced expression of a subset of TLR-dependent genes was not due to the impaired IL-10 production in IκBNS$^{-/-}$ mice.

Prolonged NF-κB Activity in IκBNS-Deficient Cells

Gene expression of *Cxcl10* (IP-10), *Ccl2* (MCP-1), and *Ccl5* (RANTES) was mainly regulated by the transcription factor IRF-3 in the TRIF-dependent pathway, whereas TNF-α, IL-6, and IL-12p40 gene expression was mainly regulated by the MyD88-dependent activation of NF-κB (Akira and Takeda, 2004; Yamamoto et al., 2003). In addition, previous in vitro studies indicated that overexpression of IκBNS leads to compromised NF-κB activity through selective association of IκBNS with p50 subunit of NF-κB (Fiorini et al., 2002; Hirotani et al., 2005). Therefore, we next analyzed LPS-induced activation of NF-κB. LPS-induced degradation of IκBα was not compromised in IκBNS$^{-/-}$ macrophages (Figure S3A). Next, peritoneal macrophages or bone marrow-derived macrophages were stimulated with LPS and DNA binding activity was analyzed by EMSA (Figure 4A; Figure S3B). LPS stimulation resulted in enhanced DNA binding activity of NF-κB in both wild-type and IκBNS$^{-/-}$ macrophages to similar extents within 1 hr. After 1 hr of LPS stimulation, NF-κB activity decreased in wild-type cells. However, NF-κB activity sustained and even at 3 hr of LPS stimulation significant DNA binding activity was still observed in

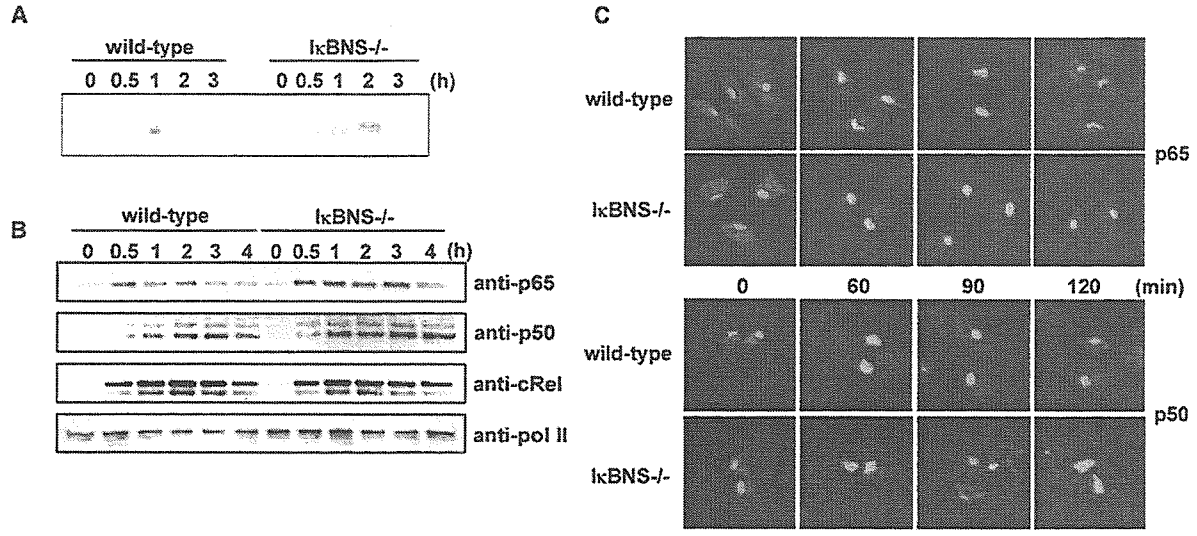

Figure 4. Persistent LPS-Induced Activation of NF-κB in IκBNS$^{-/-}$ Macrophages

(A) Peritoneal macrophages from wild-type and IκBNS$^{-/-}$ mice were stimulated with 100 ng/ml LPS. At the indicated time points, nuclear extracts were prepared, and NF-κB activation was analyzed by EMSA using a NF-κB specific probe.

(B) Peritoneal macrophages were stimulated with LPS. At the indicated time points, nuclear fractions were isolated and subjected to Western blotting using anti-p65 Ab, anti-p50 Ab, anti-cRel Ab, or anti-polII Ab.

(C) Macrophages were stimulated with LPS for the indicated periods. Then, cells were stained with anti-p65 Ab or anti-p50 Ab (red) as well as DAPI (blue), and analyzed by confocal microscopy. Merged images are shown.

IκBNS$^{-/-}$ cells. We next analyzed nuclear localization of NF-κB subunits. Peritoneal macrophages were stimulated with LPS for the indicated periods, and nuclear fractions were analyzed for expression of p65, p50, and c-Rel by immunoblotting (Figure 4B). In wild-type macrophages, nuclear translocation of p65 was observed within 30 min of LPS stimulation, and nuclear localized p65 gradually decreased thereafter. In contrast, nuclear localized p65 was still significantly observed even at 3 hr of LPS stimulation in IκBNS$^{-/-}$ cells. In addition, sustained nuclear localization of p50, but not c-Rel, was observed in IκBNS$^{-/-}$ macrophages (Figure 4B). Nuclear localization of NF-κB subunits was also analyzed by immunofluorescent staining of macrophages (Figure 4C). Without stimulation, p65 and p50 were localized in the cytoplasm, but not in the nucleus, in both wild-type and IκBNS$^{-/-}$ macrophages. LPS stimulation resulted in nuclear staining of both p65 and p50 at 1 hr. Nuclear staining of p65 and p50 gradually decreased after 1 hr of LPS stimulation and was only faintly observed at 2 hr of stimulation in wild-type cells. However, nuclear localization of p65 and p50 was still evident at 2 hr of LPS stimulation in IκBNS$^{-/-}$ cells. These findings indicate that LPS-induced NF-κB activity was prolonged in IκBNS$^{-/-}$ macrophages. NF-κB activity is terminated by degradation of promoter-bound p65 (Natoli et al., 2005; Saccani et al., 2004). We used RAW264.7 macrophage cell line and performed pulse-chase experiments with ^{35}S-labeled amino acids to analyze p65 turnover (Figure S3C). In these cells, labeled p65 was accumulated into the nucleus until 2 hr of LPS stimulation, and then p65 was degraded. In RAW cells constitutively expressing IκBNS, nuclear accumulation of labeled p65 was similarly observed until 1 hr of LPS stimulation. However, the p65 turnover was observed more rapidly and labeled p65 disappeared at 2 hr after LPS stimulation (Figure S3C). These findings indicate that IκBNS mediates the degradation of p65. The MyD88-dependent pathway mediates activation of MAP kinase cascades as well as NF-κB activation. Therefore, LPS-induced phosphorylation of p38, ERK1, ERK2, and JNK was analyzed by Western blotting (Figure S3D). LPS-induced activation of these MAP kinases was not compromised in IκBNS$^{-/-}$ macrophages.

Regulation of p65 Activity at the IL-6 Promoter by IκBNS

We next addressed how IκBNS selectively downregulates induction of genes that are induced late. We utilized the IL-6 and TNF-α promoters, which are representatives of genes activated late and early, respectively. Wild-type macrophages were stimulated with LPS and analyzed for recruitment of endogenous IκBNS to the promoters by chromatin immunoprecipitation (ChIP) assay (Figure 5A). Consistent with previous findings using IκBNS overexpressing macrophage cell lines (Hirotani et al., 2005), endogenous IκBNS was recruited to the IL-6 promoter, but not the TNF-α promoter, in LPS-stimulated macrophages. We next addressed LPS-induced recruitment of p65 to the promoters in wild-type and IκBNS$^{-/-}$ macrophages (Figure 5B). Recruitment of p65 to the TNF-α promoter peaked at 1 hr of LPS stimulation and gradually decreased thereafter in a similar manner in both wild-type and IκBNS$^{-/-}$ cells. Recruitment of p65 to the IL-6 promoter was observed to similar extents until 3 hr of LPS stimulation in wild-type and IκBNS$^{-/-}$ macrophages. After that, it decreased in wild-type macrophages. In contrast, p65 recruitment was still evident, rather enhanced, even after 5 hr of LPS stimulation in IκBNS$^{-/-}$ macrophages. Thus, p65 activity at

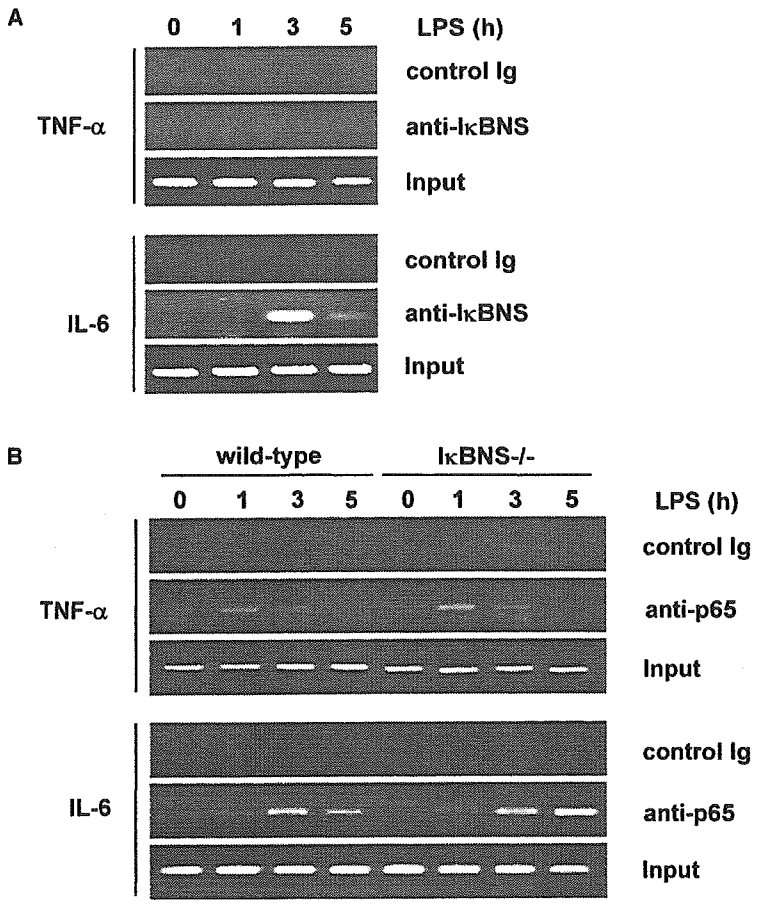

Figure 5. IκBNS Regulation of p65 Activity at the IL-6 Promoter

(A) Wild-type bone marrow-derived macrophages were stimulated with 100 ng/ml of LPS for the indicated periods, and chromatin immunoprecipitation (ChIP) assay was performed with anti-IκBNS Ab or control Ig. The immunoprecipitated TNF-α promoter (upper panel) or IL-6 promoter (lower panel) was analyzed by PCR with promoter-specific primers. PCR amplification of the total input DNA in each sample is shown (Input). Representative of three independent experiments. The same result was obtained when peritoneal macrophages were used.

(B) Macrophages from wild-type or IκBNS$^{-/-}$ mice were stimulated with LPS for the indicated periods. Then, ChIP assay was performed with anti-p65 Ab or control Ig. The immunoprecipitated TNF-α promoter (upper panel) or IL-6 promoter (lower panel) was analyzed by PCR with promoter-specific primers. Representative of three independent experiments.

the IL-6 promoter, but not at the TNF-α promoter, was prolonged in LPS-stimulated IκBNS$^{-/-}$ macrophages. Taken together, these findings indicate that TLR-inducible IκBNS is responsible for termination of NF-κB activity through its recruitment to specific promoters.

High Sensitivity to LPS-Induced Endotoxin Shock in IκBNS-Deficient Mice

To study the in vivo role of IκBNS, we examined LPS-induced endotoxin shock. Intraperitoneal injection of LPS resulted in marked increases in serum concentrations of TNF-α, IL-6, and IL-12p40 (Figure 6A). TNF-α level was comparable between wild-type and IκBNS$^{-/-}$ mice, which rapidly peaked at around 1.5 hr of LPS administration. In the case of IL-6 and IL-12p40 levels, concentrations of both cytokines were almost equally elevated within 3 hr of LPS injection. After 3 hr, levels of both cytokines gradually decreased in wild-type mice. However, concentrations of IL-6 and IL-12p40 sustained, rather enhanced, in IκBNS$^{-/-}$ mice after 3 hr. Thus, persistently high concentrations of LPS-induced serum IL-6 and IL-12p40 were observed in IκBNS$^{-/-}$ mice. Furthermore, high sensitivity to LPS-induced lethality was observed in IκBNS$^{-/-}$ mice (Figure 6B). All IκBNS$^{-/-}$ mice died within 4 days of LPS challenge at a dose of which almost all wild-type mice survived over 4 days. These findings indicate that IκBNS$^{-/-}$ mice are highly sensitive to LPS-induced endotoxin shock.

High Susceptibility to DSS-Induced Colitis in IκBNS$^{-/-}$ Mice

In a previous report, IκBNS was shown to be constitutively expressed in macrophages residing in the colonic lamina propria, which explains one of the mechanisms for hyporesponsiveness to TLR stimulation in these cells (Hirotani et al., 2005). Therefore, we next stimulated CD11b^{+} cells isolated from the colonic lamina propria with LPS and analyzed for production of TNF-α and IL-6 (Figure S4). In CD11b^{+} cells from wild-type mice, LPS-induced production of these cytokines was not significantly observed. In cells from IκBNS$^{-/-}$ mice, IL-6 production was increased even in the absence of stimulation, and LPS stimulation led to markedly enhanced production of IL-6, but not TNF-α. In the next experiment, in order to expose these cells to microflora and cause intestinal inflammation, mice were orally administered with dextran sodium sulfate (DSS), which is toxic to colonic epithelial cells and therefore disrupts the epithelial cell barrier (Kitajima et al., 1999). IκBNS$^{-/-}$ mice showed more severe weight loss compared with wild-type mice (Figure 7A). Histological analyses of the colon indicated that the inflammatory lesions were more severe and more extensive in IκBNS$^{-/-}$ mice (Figures 7B and 7C). Thus, IκBNS$^{-/-}$ mice are highly susceptible to intestinal inflammation. Th1-oriented CD4^{+} T cell response was shown to be associated with DSS colitis (Strober et al., 2002). Therefore, we analyzed IFN-γ

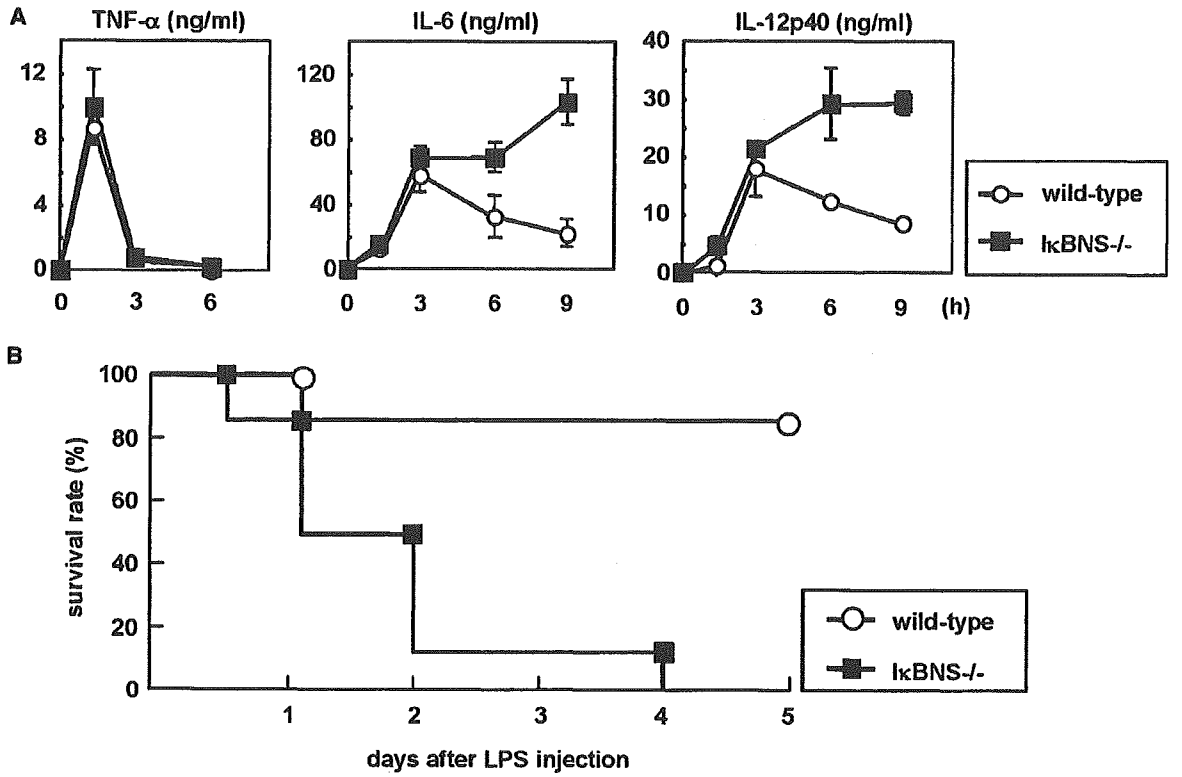

Figure 6. High Susceptibility to LPS-Induced Endotoxin Shock in IκBNS$^{-/-}$ Mice

Age-matched wild-type (n = 6) and IκBNS−/− (n = 6) mice were intraperitoneally injected with LPS (1 mg). (A) Sera were taken at 1.5, 3, 6, and 9 hr after LPS injection. Serum concentrations of TNF-α, IL-6, and IL-12p40 were determined by ELISA. Results are shown as mean ± SD of serum samples from six mice. (B) Survival was monitored for 5 days.

production from splenic CD4$^+$ T cells of wild-type and IκBNS$^{-/-}$ mice before and after DSS administration (Figure 7D). DSS administration led to a mild increase in IFN-γ production in wild-type mice. In nontreated IκBNS$^{-/-}$ mice, IFN-γ production was slightly increased compared with nontreated wild-type mice. In DSS-fed IκBNS$^{-/-}$ mice, a significant increase in IFN-γ production was observed compared to DSS-fed wild-type mice. These results indicate that IκBNS$^{-/-}$ mice are susceptible to intestinal inflammation caused by exposure to microflora.

Discussion

In the present study, we characterized the physiological function of IκBNS. Induced by TLR stimulation, IκBNS is involved in termination of NF-κB activity and thereby inhibits a subset of TLR-dependent genes that are induced late through MyD88-dependent NF-κB activation. Accordingly, IκBNS$^{-/-}$ mice show sustained production of IL-6 and IL-12p40, resulting in high susceptibility to LPS-induced endotoxin shock. Furthermore, IκBNS$^{-/-}$ mice are susceptible to intestinal inflammation accompanied by enhanced Th1 responses.

IκBNS was originally identified as a molecule that mediates negative selection of thymocytes (Fiorini et al., 2002). However, IκBNS$^{-/-}$ mice did not show any defect in T cell development. Requirement of IκBNS in negative selection of thymocytes should be analyzed precisely using peptide-specific TCR transgenic mice, such as mice bearing the H-Y TCR, in the future (Kisielow et al., 1988).

Recent studies have established that TLR-dependent gene induction is regulated mainly by NF-κB and IRF families of transcription factors (Akira and Takeda, 2004; Honda et al., 2005; Takaoka et al., 2005). In TLR4 signaling, the TRIF-dependent pathway is responsible for induction of IFN-β and IFN-inducible genes through activation of IRF-3, whereas the MyD88-dependent pathway mediates induction of several NF-κB dependent genes (Beutler, 2004). A study with mice lacking IκBζ, another member of nuclear IκB proteins, has demonstrated that the MyD88-dependent genes are divided into at least two types; one is induced early and independent of IκBζ, and another is induced late and dependent on IκBζ (Yamamoto et al., 2004). The IκBζ-regulated genes include IL-6, IL-12p40, IL-18, and G-CSF, which are all upregulated in LPS-stimulated IκBNS$^{-/-}$ macrophages. Thus, IκBNS seems to possess a function quite opposite to IκBζ. IκBNS is most structurally related to IκBζ (Fiorini et al., 2002; Hirotani et al., 2005). But, IκBζ has an additional N-terminal structure, which seemingly mediates the induction of target genes (Motoyama et al., 2005). Thus, nuclear IκB proteins IκBζ and IκBNS positively and negatively regulate a subset of TLR-induced NF-κB-dependent genes, respectively.

Recently, negative regulation of TLR-dependent gene induction was extensively analyzed (Liew et al., 2005).